

# Perturbation Analysis of the Voltage-sensitive Conformational Changes of the Na<sup>+</sup>/Glucose Cotransporter

DONALD D.F. LOO,<sup>1</sup> BRUCE A. HIRAYAMA,<sup>1</sup> ALBERT CHA,<sup>1,2</sup> FRANCISCO BEZANILLA,<sup>1,2</sup>  
and ERNEST M. WRIGHT<sup>1</sup>

<sup>1</sup>Department of Physiology and <sup>2</sup>Department of Anesthesiology, David Geffen School of Medicine at UCLA, Los Angeles, CA 90095

**ABSTRACT** Conformational changes of the human Na<sup>+</sup>/glucose cotransporter (hSGLT1) were studied using voltage-jump methods. The cotransporter was expressed in *Xenopus laevis* oocytes, and SGLT1 charge movements were measured in the micro- to millisecond time scale using the cut-open oocyte preparation and in the millisecond to second time scale using the two-electrode voltage clamp method. Simultaneous charge and fluorescence changes were studied using tetramethylrhodamine-6-maleimide-labeled hSGLT1 Q457C. In 100 mM external [Na<sup>+</sup>], depolarizing voltage steps evoked a charge movement that rose initially to a peak (with time constant  $\tau = 0.17$  ms) before decaying to steady state with two time constants ( $\tau = 2\text{--}30$  and  $25\text{--}150$  ms). The time to peak (0.9 ms) decreased with [Na<sup>+</sup>], and was not observed in 0 mM [Na<sup>+</sup>]. In absence of Na<sup>+</sup>, charge movement decayed monotonically to steady state with three time constants (0.2, 2, and 150 ms). Charge movement was accompanied by fluorescence changes with similar time courses, indicating that global conformational changes monitored by charge movement are reflected by local environmental changes at or near Q457C. Our results indicate that the major voltage-dependent step of the Na<sup>+</sup>/glucose transport cycle is the return of the empty carrier from inward to outward facing conformations. Finally, we observed subtle differences between time constants for charge movement and for optical changes, suggesting that optical recordings can be used to monitor local conformational changes that underlie the global conformational changes of cotransporters.

**KEY WORDS:** Na<sup>+</sup>/glucose cotransport • presteady-state kinetics • charge movement • fluorescence • conformational changes

## INTRODUCTION

The Na<sup>+</sup>/glucose cotransporter (SGLT1) is a member of a large family of proteins that uses the electrochemical potential gradient of Na<sup>+</sup> to accumulate substrates into cells. Cotransport occurs by an alternating access mechanism via a series of conformational changes induced by substrate binding and membrane voltage (Parent et al., 1992; Hazama et al., 1997; Loo et al., 1998; Meinild et al., 2002). A simplified six-state kinetic model has been proposed to account for the kinetics of SGLT1 (Parent et al., 1992; Hazama et al., 1997; Loo et al., 1998; Mackenzie et al., 1998; Meinild et al., 2002). The transporter has six kinetic states consisting of the ligand-free (C<sub>1</sub>, C<sub>6</sub>), Na<sup>+</sup>-bound (C<sub>2</sub>, C<sub>5</sub>), and Na<sup>+</sup>- and sugar-bound (C<sub>3</sub>, C<sub>4</sub>) states at the external and internal membrane surfaces (see Fig. 15 A). Two external Na<sup>+</sup> ions bind to the transporter before glucose, and the substrates are transported simultaneously, and glucose is released before Na<sup>+</sup> on the inside. The model accounted not only for the steady-state kinetics of SGLT1, but also predicted presteady-state transients associated with the transporter in the absence of glucose (Parent et al., 1992; Loo et al., 1993). In the model, the protein is negatively charged (valence of  $-2$ ), and membrane

voltage is assumed to influence: (a) the reorientation of the ligand-free or empty carrier between inward and outward facing conformations, and (b) the binding of external Na<sup>+</sup> to a site in the membrane electric field. Thus, there is a predicted charge movement associated with the voltage-dependent partial reactions C<sub>1</sub>↔C<sub>6</sub> (empty carrier alternating between outward and inward facing conformations) and C<sub>2</sub>↔C<sub>1</sub> (external Na<sup>+</sup> binding/dissociation).

In 1993, we reported transporter capacitive currents, carrier currents, with stepped jumps in membrane voltage (in the presence of Na<sup>+</sup> but absence of sugar), and hypothesized that most of these voltage-dependent transient currents (presteady-state currents or charge movement) are due to the voltage-sensitive conformational changes of the membrane protein (Loo et al., 1993). These presteady-state currents have been used to gain insight into the partial reactions of cotransporters (for reviews see Loo et al., 2002; Forster et al., 2002), and to estimate the total number of transporters in the cell membrane (Zampighi et al., 1995). The origin of the cotransporter transients, however, has been questioned,

*Abbreviations used in this paper:* au, arbitrary unit of fluorescence intensity; SGLT1, Na<sup>+</sup>/glucose cotransporter; TMR6M, tetramethylrhodamine-6-maleimide.

Correspondence to Donald Loo: dloo@mednet.ucla.edu

and it has been proposed that the currents are due solely to ion binding to sites within the membrane electric field (e.g., Su et al., 1996).

By combining presteady-state measurements with optical techniques using extrinsic fluorescent probes covalently bound to engineered cysteine residues in the transporter (Loo et al., 1998; Meinild et al., 2002), we have established that the presteady-state currents of SGLT1 are due to  $\text{Na}^+$  binding/dissociation and transitions of the empty transporter between outward- and inward-facing conformations (Loo et al., 1998; Meinild et al., 2002). We have also shown that the fluorescent changes in the tetramethylrhodamine-6-maleimide (TMR6M)-labeled hSGLT1 mutant Q457C reports local conformational changes (at Cysteine 457) associated with ligand binding ( $\text{Na}^+$  and sugar) and voltage jumps.

In this study using both charge and fluorescence measurements, we have set out to extend the voltage- and  $\text{Na}^+$ -induced perturbations in the conformation of SGLT1 over a wider time scale, ranging from microseconds to seconds. Our previous studies have examined the conformational changes of SGLT1 with time constants in the range of 3–35 ms. The motivations for performing charge and fluorescence measurements at an expanded time scale were our simulations on the six-state kinetic model for SGLT1, which predicted a fast rising phase of charge movement with depolarizing potentials (Parent et al., 1992; Hazama et al., 1997), and our observation that steady-state conditions are not reached at the end of our standard 100-ms voltage pulses.

The concurrent employment of an independent optical method to monitor voltage-induced conformational changes in the transporter overcomes some of the inherent limitations of charge measurements alone. Our results demonstrate that there are at least three components of voltage-induced perturbations in hSGLT1 with time constants ranging from 0.2 to 200 ms. The slow ( $\tau = 30\text{--}200$  ms) and medium (3–20 ms) components contribute equally to total charge transfer, while the fast (0.2–1.5 ms) component contributes the most to total fluorescence changes. Under  $\text{Na}^+$ -free conditions, all three components are still evident, but the time constants decrease in magnitude. We conclude that most of the SGLT1 charge movement is due to the reorientation of intrinsic charge in the membrane protein and that there are at least two intermediate conformations ( $C_{1a}$  and  $C_{1b}$ ) between the two final states  $C_1$  and  $C_6$  in the external and internal membrane surfaces ( $C_1 \leftrightarrow C_{1a} \leftrightarrow C_{1b} \leftrightarrow C_6$ ). External  $\text{Na}^+$  modulates charge transfer between  $C_1$  and  $C_6$  by increasing the occupancy of the  $\text{Na}^+$ -bound state ( $C_2 = C_1\text{Na}_2$ ) and reducing the occupancies of  $C_1$ ,  $C_{1a}$ ,  $C_{1b}$ , and  $C_6$ . This suggests that  $C_1$  is meta-stable; the highest probability

states are  $C_2$  in the presence of  $\text{Na}^+$ , and  $C_6$  in the absence of  $\text{Na}^+$ . The implication is that after the  $\text{Na}^+$ /glucose transport step, the high external  $\text{Na}^+$  concentration shifts the transporter from the cytoplasm ( $C_6$ ) into the state with the highest affinity for glucose ( $C_2$ ) to initiate another cycle of  $\text{Na}^+$ /glucose transport across the membrane. Our results also suggest that the voltage sensitivity of  $\text{Na}^+$ /glucose cotransport resides mainly in return of the empty carrier from the inward- to outward-facing conformation ( $C_6$  to  $C_1$ ).

## MATERIALS AND METHODS

### Strategy

Our general strategy was to express SGLTs in *Xenopus laevis* oocytes and to record changes in transporter currents and extrinsic fluorescence over a wide time scale (microsecond to seconds) after rapid jumps in the membrane potential. In the absence of sugar, the transient transporter currents are capacitive, due to a reorientation of the protein charge in the membrane electric field, and/or the binding and dissociation of external  $\text{Na}^+$  in a well within the membrane field. To examine the role of  $\text{Na}^+$ , external  $[\text{Na}^+]$  was varied between 0 and 100 mM by isomolar replacement of NaCl with cholineCl.  $\text{Na}^+$  binding and dissociation at the cytoplasmic face of the protein may be neglected as the cytoplasmic concentration is either low ( $\sim 10$  mM in intact oocytes) or absent in the cut-open oocyte preparation (see below) and the internal  $\text{Na}^+$  binding affinity is low (Eskandari et al., 1999; Sauer et al., 2000; Quick et al., 2003).

The two-electrode voltage clamp, with a settling time 0.6–1.0 ms (Loo et al., 1993), was used to record transients in the millisecond to second range. To examine kinetic events in the microsecond to millisecond range, the cut-open oocyte preparation, with a settling time of 80  $\mu\text{s}$  (Tagliatalata et al., 1992; Stefani and Bezanilla, 1998) was used. The wild-type human SGLT1 (hSGLT1) was used to record transporter charge movements, and the hSGLT1 mutant transporter, Q457C, was used to correlate fluorescence and charge movement (Loo et al., 1998; Meinild et al., 2002). Previously, it has been shown that the mutant protein is able to transport sugar, but sugar transport is abolished on alkylation of Cys457 with methanethiosulfonate reagents, or after labeling by TMR6M (Loo et al., 1998; Meinild et al., 2002). Since the TMR6M-labeled mutant transporter can bind  $\text{Na}^+$  and sugar, it can be used for studying the conformational changes associated with ligand binding and voltage jumps. The human isoform was used because the distribution of the protein between outside-facing and inside-facing conformations was at a midpoint at the normal resting potential (holding potential) of the oocyte,  $-50$  mV. This means that over the practical range of voltage jumps that can be used with oocytes,  $-150$  to  $+50$  mV, the full charge movement may be recorded by hyperpolarizing the membrane to  $-150$  mV and depolarizing to  $+50$  mV. It should also be borne in mind that the midpoint  $V_{0.5}$  for SGLT1 shifts by  $\sim 100$  mV per 10-fold reduction in external  $[\text{Na}^+]$  (Loo et al., 1993; Hazama et al., 1997; Quick et al., 2001), and this means that it is not feasible to obtain the full charge vs. voltage curve at  $[\text{Na}^+] < 10$  mM.

### Preparation and Maintenance of Oocytes

Mature *Xenopus laevis* oocytes were isolated, defolliculated, injected with human SGLT1 or human SGLT1 Q457C cRNA (Loo et al., 1993, 1998). hSGLT1 Q457C was labeled with 200  $\mu\text{M}$  TMR6M (Loo et al., 1998).

## Combined Electrophysiological and Fluorescence Experiments

Electrophysiological and fluorescence experiments were performed simultaneously, using either two-electrode (Loo et al., 1998; Meinild et al., 2001) or cut-open oocyte voltage clamp fluorometry (Cha and Bezanilla, 1997, 1998). The current records were the averages of 3–4 sweeps, and the fluorescence records were averages of either 4 or 20 sweeps. Interpulse interval was  $\geq 1$  s. Records were filtered at 2 kHz, 500 Hz, or 50 Hz, depending on the sampling interval (5  $\mu$ s to 750  $\mu$ s per sample). In two-electrode voltage clamp experiments, the bath contained 100 mM NaCl buffer (in mM, 100 NaCl, 2 KCl, 1 CaCl<sub>2</sub>, 1 MgCl<sub>2</sub>, 10 HEPES, pH 7.4). In cut-open oocyte experiments, external and guard solutions contained (in mM) 100 Na-methanesulfonate, 1 CaCl<sub>2</sub>, 10 HEPES (pH 7.3), and internal solution contained (in mM) 100 K-methanesulfonate, 1 EGTA, 10 HEPES (pH 7.3). The Na<sup>+</sup> concentration was varied by equimolar replacement of Na<sup>+</sup> with choline. Fluorescence data have been corrected for rundown (Meinild et al., 2002). All experiments were performed at room temperature (20–23°C).

## Data Analysis

**Isolation of Presteady-state Currents.** In response to a voltage pulse, the total membrane current consisted of the membrane bilayer capacitive transient, the presteady-state currents of SGLT1, and the steady-state current. Using 100-ms voltage pulses, we have reported that the relaxation of the presteady-state current exhibited a single time constant between 2 and 30 ms (Loo et al., 1993; Hazama et al., 1997; Quick et al., 2001; Meinild et al., 2002). In pilot studies, we found additional components with time constants between 0.2–2 and 35–160 ms. For clarity of presentation, we operationally defined the fast, medium, and slow components (for charge and fluorescence) as those with time constants between 0.2–2, 2–20, and 30–160 ms, respectively. Since at each voltage step their time constants differed by an order of magnitude, the components were estimated separately using test voltage pulses of different durations.

**Slow Component.** The time constant of the slow component was estimated from the current relaxations after the medium component has decayed. The early phase was obtained by extrapolation of the exponential fit to the peak of the capacitive transient, typically two sample points after onset of the voltage pulse. The slow charge was obtained from the integral of the slow component of presteady-state current.

**Medium Component.** The medium component was estimated using 100-ms voltage pulses after subtraction for the slow component (above) and the steady-state current. The compensated current was fitted to the function

$$I(t) = I_{\text{cm}} \exp(-t/\tau_{\text{cm}}) + I_{\text{med}} \exp(-t/\tau_{\text{med}}),$$

where  $I_{\text{cm}} \exp(-t/\tau_{\text{cm}})$  is, to a first approximation, the capacitive current. The charge was obtained from the integral of the medium component.

**Phlorizin Subtraction.** An alternative procedure for isolating the SGLT1 transient was to use phlorizin subtraction (Loo et al., 1993; Hazama et al., 1997; Meinild et al., 2001). The transients were obtained by pointwise-subtraction of the current relaxations in 100  $\mu$ M external phlorizin (in the presence of Na<sup>+</sup>) from those obtained in the absence of phlorizin (in Na<sup>+</sup>). In Na<sup>+</sup>-free situations (e.g., Fig. 5, C and D), they were obtained by subtraction of the current relaxations in 100  $\mu$ M phlorizin and 100 mM Na<sup>+</sup> from the current relaxations in 0 mM Na<sup>+</sup>. The currents isolated by phlorizin subtraction were the total presteady-state currents. Subtraction could not be used with the TMR6M Q457C be-

cause of the low phlorizin affinity ( $K_i \approx 100$   $\mu$ M for TMR6M Q457C vs. 200 nM for hSGLT1).

**Cut-open Oocyte Experiments.** The background leak currents and the oocyte bilayer capacitive transients were first compensated with the voltage clamp amplifier (CA-1; Dagan Corporation). The P/4 protocol was used to isolate the presteady-state currents (Bezanilla and Armstrong, 1977; Bezanilla and Stefani, 1998) using a subtracting holding potential ( $V_{\text{shp}}$ ) of  $-150$  mV where there was negligible SGLT1 charge movement.<sup>1</sup>

**Fitting of  $Q$ - $V$  and  $\Delta F$ - $V$  Relations.** The charge vs. voltage ( $Q$ - $V_m$ ) relations could, to a first approximation, be fitted to a single Boltzmann function (Loo et al., 1993; Hazama et al., 1997):

$$(Q - Q_{\text{hyp}})/Q_{\text{max}} = 1/[1 + \exp(z\delta(V_m - V_{0.5})/RT)],$$

where  $Q_{\text{max}} = Q_{\text{dep}} - Q_{\text{hyp}}$ ,  $Q_{\text{dep}}$  and  $Q_{\text{hyp}}$  are the  $Q$  (absolute value) at depolarizing and hyperpolarizing limits,  $V_m$  is membrane potential,  $F$  is the Faraday,  $R$  is the gas constant,  $T$  is the absolute temperature,  $V_{0.5}$  is the membrane potential at 50%  $Q_{\text{max}}$  (or the midpoint voltage),  $z$  is apparent valence of the movable charge, and  $\delta$  is the fraction of the membrane electric field traversed by the charge.  $z\delta$  is the steepness factor for the dependence of  $Q$  on voltage. The Boltzmann relation was also used to fit the dependence of the change of fluorescence intensity ( $\Delta F$ ) on membrane voltage (Loo et al., 1998; Meinild et al., 2002). The parameters obtained were the maximal fluorescence intensity change ( $\Delta F_{\text{max}}$ ), the membrane voltage at 50%  $\Delta F_{\text{max}}$  ( $V_{0.5}$ ), and the product ( $z\delta$ ) of the apparent valence of the fluorescence voltage sensor ( $z$ ) and the dielectric distance ( $\delta$ ).

Fits of data to equations were performed using either SigmaPlot 2002 (SPSS) or Clampfit 8.1 (Axon Instruments). Unless otherwise noted, statistics were obtained from the error of the fit. While data are shown for representative experiments, all experiments were performed on at least three oocytes from different batches.

## RESULTS

### Part I. Charge Movement

The first part describes the time course of voltage-induced capacitance currents (the presteady-state current) through SGLT1. The study extends our previous experiments to encompass sub-millisecond and second time domains. Charge measurements are presented for wild-type human SGLT1 and the TMR6M-labeled hSGLT1 mutant Q457C. The latter was used to monitor the conformational changes of the transporter by fluorescence measurements.

**Slow and Medium Charge Movements in hSGLT1.** The raw current records from an oocyte expressing hSGLT1 performed with the two-electrode voltage clamp are shown in Fig. 1 A. The membrane potential was held at  $-50$  mV ( $V_h$ ) and stepped to a test value ( $V_t$ , from  $+50$  to  $-150$  mV, and representative traces are shown) for

<sup>1</sup>Since the  $V_{0.5}$  for charge is very negative in the absence of Na ( $\sim -200$  mV), some SGLT charge is being subtracted using the P/4 protocol. However, it does not invalidate the conclusions of the present study because the time course of the fast charge movement was not altered since the time constants were independent of voltage (Fig. 6 C).

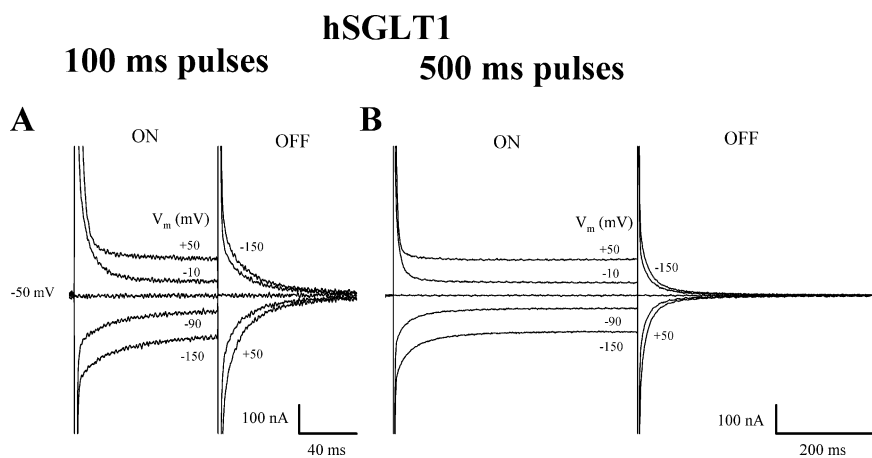


FIGURE 1. Time course of the raw or total currents (capacitive and hSGLT1 presteady-state currents) of an oocyte expressing hSGLT1. The experiment was performed using a two-electrode voltage clamp, and all data were obtained from a single oocyte. Membrane potential was held at  $-50$  mV ( $V_h$ ) and then stepped to a series of test values  $V_t$  (from  $+50$  to  $-150$  mV in  $20$ -mV decrements; representative traces are shown for  $+50$ ,  $-10$ ,  $-50$ ,  $-90$ , and  $-150$  mV) before returning to  $V_h$ . The pulse duration was  $100$  ms in A and  $500$  ms in B, and the currents, which are the average of three sweeps, have been filtered at  $500$  Hz (A) and  $50$  Hz (B). An upwards deflection of the current trace represents an outward current.

$100$  ms before returning to  $V_h$ . The current contained (a) an initial spike, with a time constant of  $0.7$ – $1.0$  ms; (b) hSGLT1 presteady-state currents, which decayed to an apparent steady state with time constants of  $3$ – $25$  ms; and (c) the steady-state current, comprising of the background current of the oocyte and a hSGLT1-mediated  $\text{Na}^+$ -uncoupled (or leak) current due to the uniporter function of the transporter in the absence of sugar (Umbach et al., 1990; Loo et al., 1999). Only the initial spike and the background currents were observed in noninjected oocytes. Inspection of the recordings on oocytes with high levels of expression reveals that the steady state has not been reached at  $100$  ms, especially in the hyperpolarizing direction (Fig. 2 A). We therefore applied voltage pulses of up to seconds in duration.

The raw current records (from the same oocyte as Fig. 1 A) for a  $500$ -ms pulse are shown in Fig. 1 B. Compared with the  $100$ -ms pulse, it was necessary to increase the sampling interval from  $0.1$  to  $0.5$  ms and to filter the current records at  $50$  Hz (vs.  $500$  Hz for the  $100$ -ms pulse). This resulted in a filtering or rounding off of the  $3$ – $25$  ms (medium) component of presteady-state current (Fig. 1 B). Steady state was reached by  $500$  ms.

The procedure for isolating the components of the presteady-state current is illustrated in Fig. 2 for the ON response. The fit of the slow component began after a period of five times the relaxation time constant of the medium component ( $\tau_{\text{med}}$ ). At  $5\tau_{\text{med}}$  (typically  $\approx 100$  ms), the medium component has decayed  $99\%$  (from the initial value), and the remaining slow relaxations were well described by a single exponential function (Fig. 2 B). Fig. 2 D shows the slow component extrapolated to the beginning of the pulse.

The medium component was obtained from the  $100$ -ms current records by first subtracting the slow component (dashed line in Fig. 2 A) from the total current, and then subtracting the membrane capacitive currents (Fig. 2 C).

Fig. 3 shows the OFF currents when the test potential was returned to  $V_h$ . The slow relaxations (between  $100$  and  $500$  ms) could be fitted by a single exponential function (Fig. 3 B). Fig. 3 (C and D) shows the isolated slow and medium components. All charge movements associated with hSGLT1 in the presence of  $\text{Na}^+$  (the medium and slow components and the rising phase described in Fig. 6 below) were blocked by  $100$   $\mu\text{M}$  phlorizin, the specific high-affinity competitive inhibitor of SGLT1 (unpublished data).

The voltage dependence of the time constant ( $\tau$ ) for the ON transient was qualitatively similar for the medium and slow components (Figs. 4 A). In the hyperpolarizing direction,  $\tau$  ( $\approx 20$  ms for the medium and  $\approx 100$  ms for the slow component) was relatively independent of voltage. In the depolarizing direction,  $\tau$  decreased as the test voltage became more positive, to  $3$  and  $30$  ms (at  $+50$  mV) for the medium and slow components, respectively. The time constant for the OFF transients when membrane was stepped from the test voltage ( $V_t$ ) back to  $V_h$  was independent of  $V_t$ . In this and subsequent figures, for simplicity, the OFF time constant is shown at  $V_m -50$  mV (open symbols in Fig. 4 A). The OFF time constants were  $15 \pm 1$  ms ( $n = 10$ ) and  $99 \pm 4$  ms ( $n = 10$ ) for the medium and slow components, respectively.

The medium ( $Q_{\text{med}}$ ) and slow charges ( $Q_{\text{slow}}$ ) were obtained by integration of the corresponding presteady-state currents for the ON and OFF responses (Fig. 2, C and D; Fig. 3, C and D). The charge vs. voltage relations ( $Q$ - $V$ ) for the medium and slow components were sigmoidal, and the ON and OFF charges were approximately equal at each test voltage (Fig. 4, B and C). The curve in Fig. 4 B was obtained from the fit of the mean of the ON and OFF charge movements for the medium component (at each  $V_t$ ) to a Boltzmann relation with  $Q_{\text{max}} = 8.7$  nC,  $z\delta = 1.0$ , and  $V_{0.5} = -33$  mV. The corresponding result for the slow component is presented in Fig. 4 C, with the curve described by

# ON

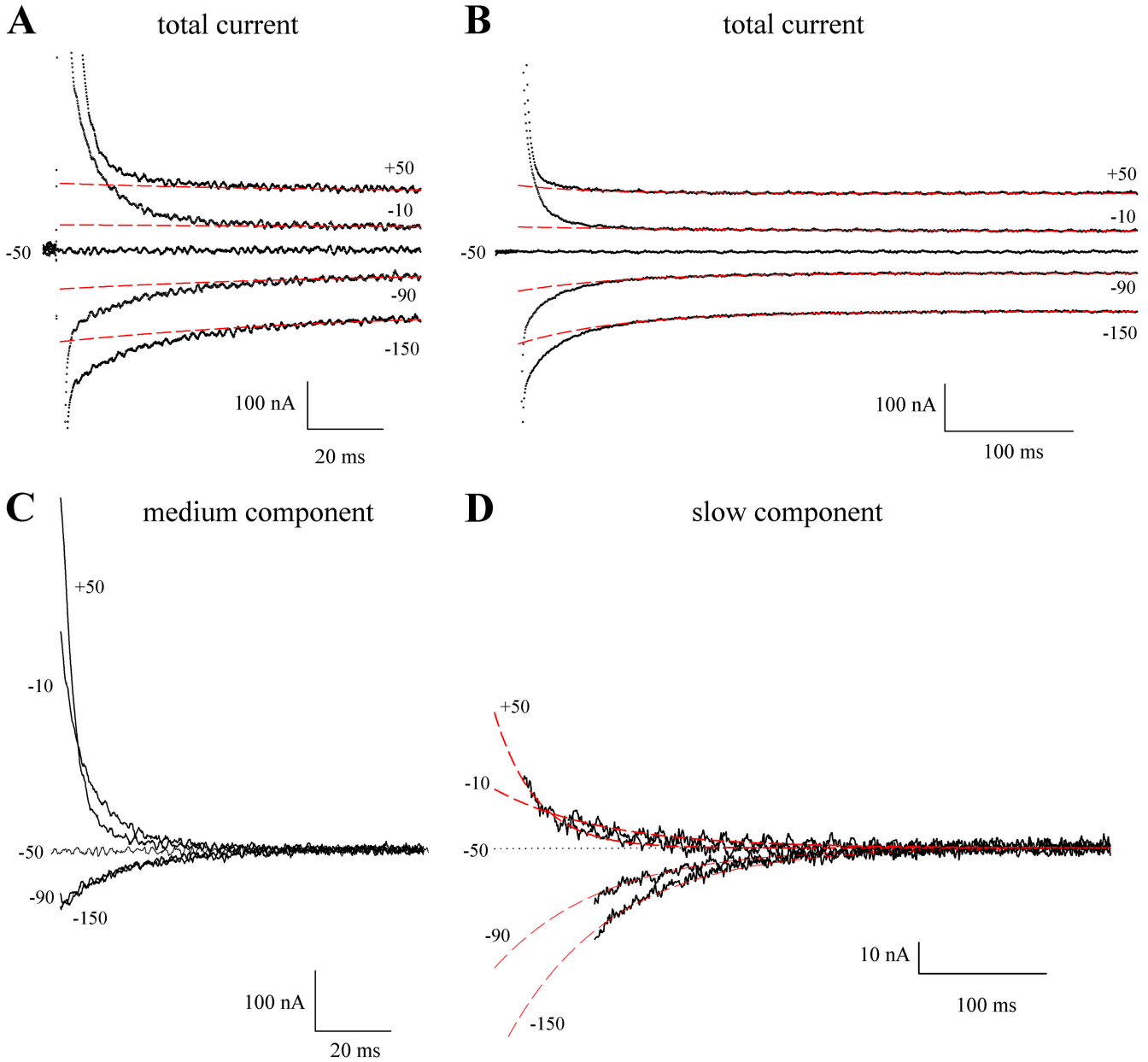


FIGURE 2. Medium and slow components of the presteady-state currents of hSGLT1 (ON response). Shown are the current records for the ON pulse from  $V_h$  ( $-50$  mV) to  $V_t$   $+50$ ,  $-10$ ,  $-50$ ,  $-90$ , and  $-150$  mV for the 100-ms (A) and the 500-ms (B) duration pulses. The data were from the same oocyte as Fig. 1. To isolate the slow charge, the steady-state current was removed, and the transient current (for the 500 ms pulses) was fitted to a single exponential function. The fit was restricted to the region between  $5\tau_{med}$  ( $\tau_{med} \approx 3$ – $20$  ms) and 500 ms. The starting point was 25 ms at  $+50$  mV, 60 ms at  $-10$  mV, and 100 ms at  $V_t$  more negative than  $-90$  mV. The fit was extrapolated to the peak of the total current trace (dashed lines in A and B), typically two data samples after onset of the voltage pulse (to 0.2 ms in A). The isolated slow charge is shown in D. To obtain the medium component, the slow component (dashed line) was subtracted from the 100-ms current records (A). The difference was fitted to  $I(t) = I_{cm} \exp(-t/\tau_{cm}) + I_{med} \exp(-t/\tau_{med})$ . Panel C shows the medium charge obtained after subtraction of the membrane capacitance ( $I_{cm} \exp(-t/\tau_{cm})$ ). For clarity, the current trace at  $-50$  mV ( $V_h$ ) has been omitted in D.

the parameters  $Q_{max} = 7.2$  nC,  $z\delta = 1.0$ , and  $V_{0.5} = -67$  mV.

The medium and slow charges ( $Q_{med}$  and  $Q_{slow}$ ) were added to obtain the total charge (Fig. 4 D). In the hyper-

polarizing direction, the total ON charge was equal in magnitude but opposite in sign to the total OFF charge. At the two most positive test voltages applied,  $+50$  and  $+30$  mV, the ON charge was slightly less than the OFF

## OFF

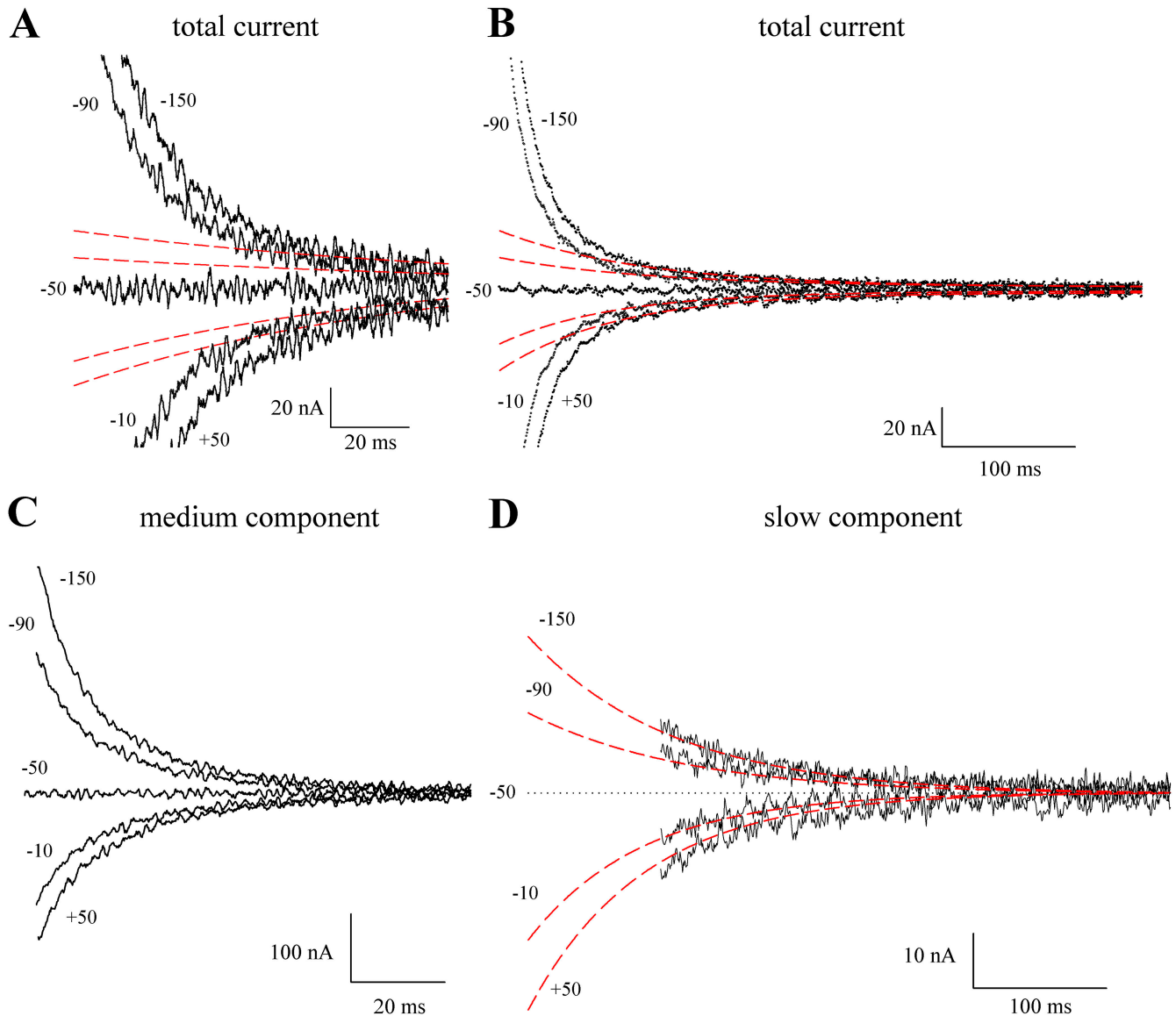


FIGURE 3. Medium and slow components of the presteady-state currents of hSGLT1 (OFF response). Shown are the current records for the OFF pulse when membrane potential was stepped from the test potential (+50, -10, -50, -90, and -150 mV) back to the holding (-50 mV) for the 100 ms (A) and the 500 ms (B) duration pulses. The data were from the same oocyte as Fig. 1, and the protocol for isolation of the medium (C) and slow components of charge movement (D) is as described in Fig. 2. As  $\tau_{\text{med}}$  for OFF was independent of test voltage ( $\tau_{\text{med}} = 15$  ms, see Fig. 4 A), the initial point for the fit (Fig. 3 B) was 96 ms for all the OFF pulses.

charge. The difference suggests that the kinetics of the ON response might be too fast to be accurately measured using the two-electrode voltage clamp (see Fig. 7). The curve in Fig. 4 D was the fit of the OFF charge to the Boltzmann relation with  $z\delta = 1.0$  and  $V_{0.5} = -44$  mV.

*Slow and Medium Charge Movements in Q457C.* Medium and slow components of charge movement were observed in the 100- and 500-ms current records of the TMR6M-labeled Q457C (unpublished data), and their characteristics were similar to those of wild-type

hSGLT1. The  $\tau$ -V relation for the medium component ( $\tau_{\text{med}}$ ) was the same as hSGLT1; for test voltages more negative than -50 mV,  $\tau_{\text{med}}$  was  $\approx 20$  ms and was independent of voltage, and in the depolarizing direction,  $\tau_{\text{med}}$  decreased to  $\approx 3$  ms at +50 mV (compare Fig. 4 A). Like wild-type hSGLT1, for hyperpolarizing voltages, the slow component of TMR6M-labeled Q457C was independent of voltage for the ON and OFF pulses. The time constant ( $\tau_{\text{slow}}$ ) ranged between 60 and 200 ms, depending on the level of expression of hSGLT1-

## hSGLT1

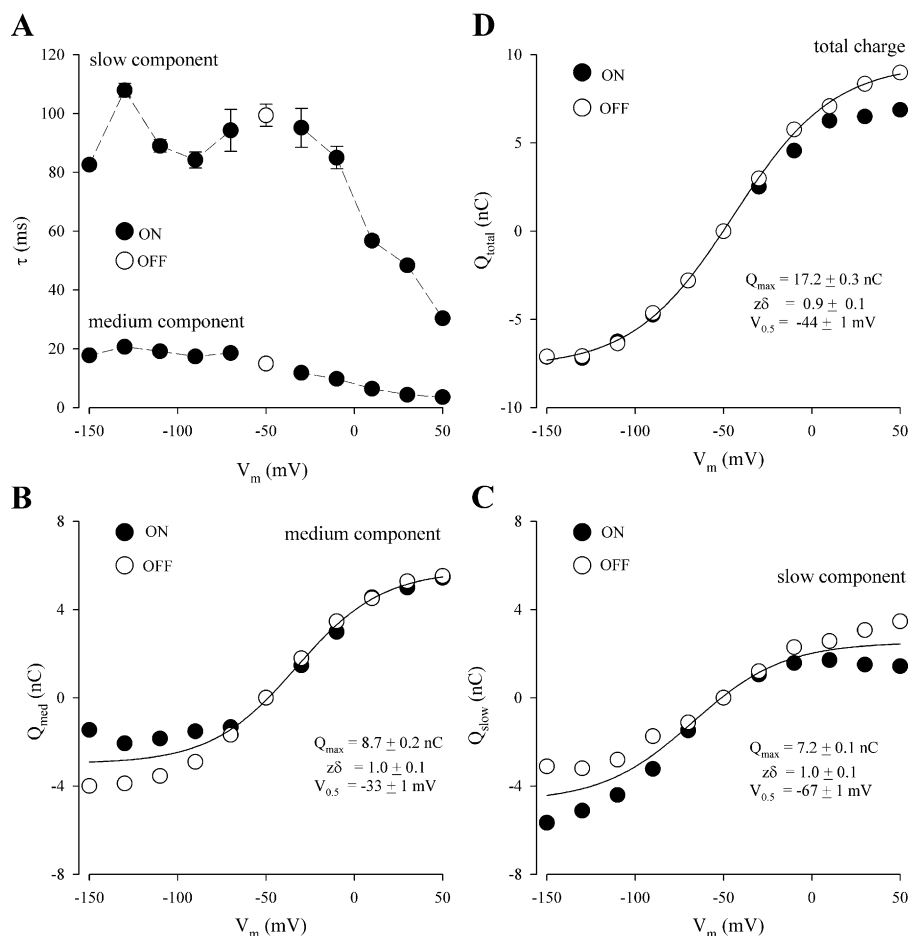


**FIGURE 4.** Kinetics of charge movement of hSGLT1: voltage dependence of the medium and slow components. Data was from the experiment of Fig. 1. (A)  $\tau$ - $V$  relations. The filled symbols represent the ON where membrane potential was stepped from  $V_h$  ( $-50$  mV) to different test potentials ( $V_t$ ). The open symbols represent the time constant of the relaxation of the OFF where membrane potential was returned from  $V_t$  to  $V_h$  ( $-50$  mV). Error bars are standard errors (SE) of the fit when the SE exceeds the size of the symbol. The OFF responses were independent of the previous test potential ( $V_t$ ), and open symbols represent the mean of 10 values with  $V_t$  varying between  $+50$  and  $-150$  mV. (B)  $Q$ - $V$  relations for the medium charge. At each  $V_m$ , the medium charge ( $Q$ ) was obtained as the time integral of the medium presteady-state current for the ON (circles) and OFF (squares) responses. The curve is the fit of the mean of the medium ON and OFF charge to the Boltzmann relation with  $Q_{\text{max}} = 8.7 \pm 0.2$  nC,  $z\delta = 1.0 \pm 0.1$ , and  $V_{0.5} = -33 \pm 1$  nC. (C)  $Q$ - $V$  relations for slow charge. Slow charge ( $Q$ ) was obtained from the time integral of the slow presteady-state current for the ON and OFF responses. The curve is the fit of the mean of the slow ON and OFF charge to the Boltzmann relation with  $Q_{\text{max}} = 7.2 \pm 0.1$  nC,  $z\delta = 1.0 \pm 0.1$ , and  $V_{0.5} = -67 \pm 1$  nC. (D)  $Q$ - $V$  relations for total charge. Total charge is the sum of the medium and slow

components (described in B and C). Filled and open symbols represent the total ON and OFF, respectively. The smooth curve is the fit of the total OFF charge to the Boltzmann relation with  $Q_{\text{max}} = 17.2 \pm 0.3$  nC,  $z\delta = 0.9 \pm 0.1$ , and  $V_{0.5} = -44 \pm 1$  mV.

Q457C; the higher the expression, the larger was  $\tau_{\text{slow}}$ . This variation in  $\tau_{\text{slow}}$  was possibly due to an underestimation of  $\tau_{\text{slow}}$  at low levels of expression seen with this mutant. As in hSGLT1, the magnitudes of the medium and slow charges for the OFF response (in TMR6M Q457C) were comparable and contributed equally to the total charge. The  $Q$ - $V$  relation for total charge could be fitted by the Boltzmann relation with  $z\delta = 1.0$  and  $V_{0.5}$  in the range  $-40$  to  $-65$  mV.

**Rising Phase of Charge Movement in hSGLT1.** At a high sampling rate ( $8 \mu\text{s}/\text{sample}$ ), we have observed a rising phase with the two-electrode voltage clamp (Fig. 5 A). In this record, the presteady-state current was obtained by phlorizin subtraction. With onset of the depolarizing voltage pulse, the current rose initially to a peak (at 1.5 ms) before decaying toward the steady state. The rising phase was not observed for hyperpolarizing voltages (Fig. 5 A).

The rising phases (at  $+50$  to  $-10$  mV) were superimposable when the current traces were normalized to

the peak current (at 1.5 ms). The current records were fitted to a sum of two exponentials with the constraint that the time constant of decay was the same as those obtained from the same oocyte with 100-ms pulses.  $\tau$  for the rising phase was  $550 \pm 60 \mu\text{s}$  ( $n = 4$ ) and was independent of test voltage ( $+50$  to  $-10$  mV).

When external  $\text{Na}^+$  concentration ( $[\text{Na}^+]_o$ ) was reduced from 100 to 12 mM, the time to peak ( $t_{\text{peak}}$ ) was reduced (Fig. 5 B). For the  $+50$  mV pulse illustrated,  $t_{\text{peak}}$  was 1.5 ms at 100 mM  $[\text{Na}^+]_o$ , 0.9 ms at 25 mM  $[\text{Na}^+]_o$ , and 0.7 ms at 12 mM  $[\text{Na}^+]_o$ . A plot of  $t_{\text{peak}}$  vs.  $[\text{Na}^+]_o$  (at 100, 50, 25, 12, and 6 mM) yielded a sigmoidal relation with a Hill coefficient between 1 and 2 (unpublished data).

From peak current, the time constant of the medium component of decay of transient current decreased with external  $\text{Na}^+$  concentration (Fig. 5 B), and this is illustrated for 100 and 0 mM  $[\text{Na}^+]_o$  in Fig. 5 C. At  $-150$  mV,  $\tau$  decreased from 18 to 3.5 ms, and from 4.5 to 1.9 ms at  $+50$  mV (see inset). In the working voltage

hSGLT1  
rising phase of charge movement

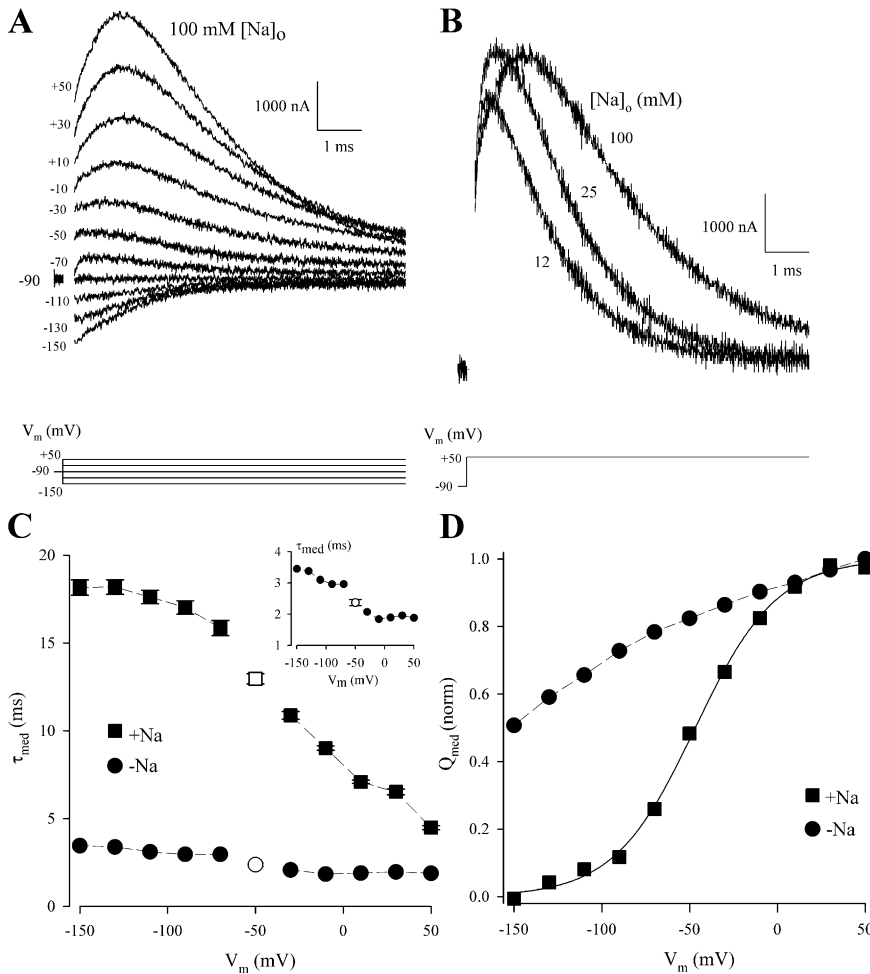


FIGURE 5. Rising phase of charge movement. The experiment was performed on hSGLT1 using a two-electrode voltage clamp. Current records were obtained by phlorizin subtraction.  $V_h$  was  $-90$  mV, data were digitized at  $8 \mu\text{s}$  per sample, and pulse was  $6$  ms. (A) Presteady-state currents in  $100$  mM  $[\text{Na}^+]_o$ . (B) Dependence of the rising phase on  $[\text{Na}^+]_o$ . The current records were obtained at  $V_t = +50$  mV in  $100$ ,  $25$ , and  $12$  mM  $[\text{Na}^+]_o$ . (C)  $\tau$ - $V$  relations for the medium component in  $100$  and  $0$  mM  $[\text{Na}^+]_o$ . Data were obtained from one oocyte. The open symbols were obtained from the OFF response and represent the mean of  $10$  values (with test potential varying between  $+50$  and  $-150$  mV). (D)  $Q$ - $V$  relations for the medium component in  $100$  and  $0$  mM  $[\text{Na}^+]_o$ .  $Q$  was obtained from the mean of the ON and OFF charges using  $100$ -ms pulses in  $100$  mM  $\text{Na}^+$  and  $30$ -ms pulses for  $0$  mM  $\text{Na}^+$ . The curve (for  $100$  mM  $\text{Na}^+$ ) was drawn using the Boltzmann relation with  $Q_{\text{max}} = -20.3 \pm 0.4$  nC,  $z\delta = 1.1 \pm 0.1$ , and  $V_{0.5} = -47 \pm 1$  mV.

range ( $+50$  to  $-150$  mV), the “maximal” charge recorded (the difference in charge between the limits  $+50$  and  $-150$  mV) was reduced  $50\%$  on removing  $\text{Na}^+$  (Fig. 5 D). We were unable to estimate the  $Q_{\text{max}}$ ,  $z\delta$ , and  $V_{0.5}$  under  $\text{Na}^+$ -free conditions because the charge did not saturate at the largest hyperpolarizing voltage applied ( $-150$  mV). This observation is in agreement with the previous finding that the midpoint voltage ( $V_{0.5}$ ) of the  $Q$ - $V$  curve (for the medium component) became more negative by  $100$  mV per  $10$ -fold decrease in  $[\text{Na}^+]_o$  (Hazama et al., 1997; Quick et al., 2001).

The cut-open oocyte voltage clamp, with a settling time of  $<80 \mu\text{s}$ , was used to examine the rising phase of charge movement in more detail. Representative current records for the hSGLT1-Q457C labeled with tetramethylrhodamine-6 maleimide (TMR6M) are shown in Fig. 6.  $V_h$  was  $-80$  mV, and the traces (shown for  $V_t$   $+50$  and  $-150$  mV) were obtained with a sampling interval of  $5 \mu\text{s}$ . In  $\text{Na}^+$ , the current rose from an initial low value (close to  $0$  nA) to a peak (at  $0.9$  ms for  $V_t$   $+50$

mV) before decaying toward steady state. The time duration at peak current was rather broad,  $\approx 0.5$ – $1$  ms. As in two-electrode voltage clamp experiments (Fig. 5 A), the rise to peak current became less pronounced as  $V_t$  was made less positive (not depicted). In the hyperpolarizing direction, the current showed a simple relaxation to steady state. In the OFF response, current decayed from an early time point (Fig. 6 A). In the absence of  $\text{Na}^+$ , the rising phase was not observed for depolarizing or hyperpolarizing pulses.

The time constants for the fast current records are shown in Fig. 6 C. In the presence of  $\text{Na}^+$ , for hyperpolarizing voltage pulses ( $-110$  to  $-130$ ), current decayed with a time constant of  $1.3 \pm 0.1$  ms ( $n = 3$ ). In the depolarizing direction, for  $V_t$  between  $-50$  and  $+50$  mV, current rose to a peak with a time constant of  $0.17 \pm 0.01$  ms ( $n = 6$ ), and then decayed with a time constant of  $\approx 3$  ms or greater (unpublished data). In the absence of external  $\text{Na}^+$ , current decayed to steady state with a voltage-independent time constant of  $0.24 \pm 0.01$  ms ( $n = 9$ ) for ON, and  $0.17 \pm 0.01$  ms for OFF.



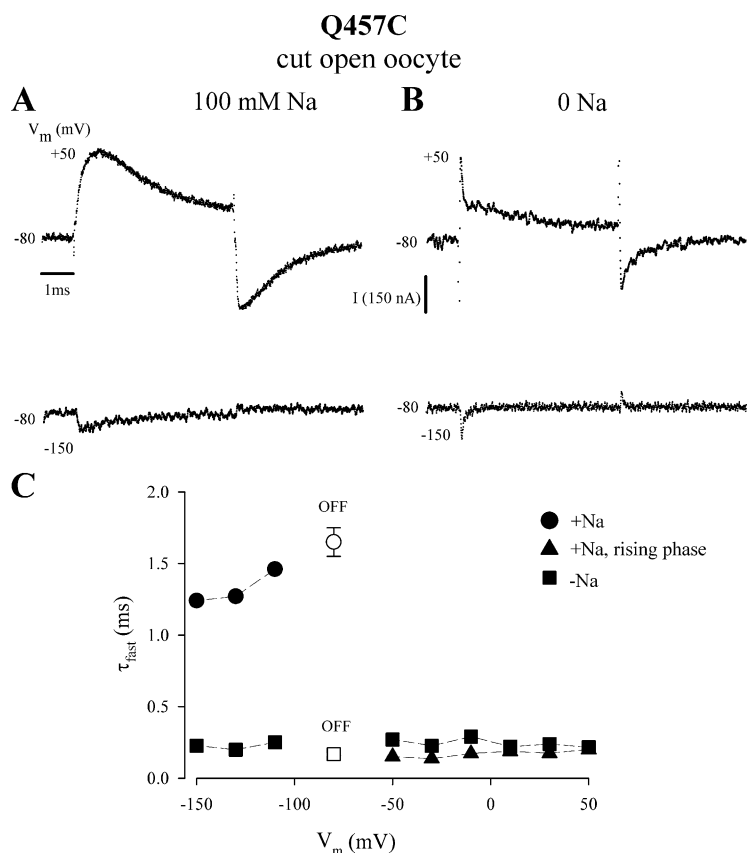


**FIGURE 6.** The rising phase of charge movement in hSGLT1-Q457C. The experiment was performed on TMR6M-labeled Q457C using the cut-open oocyte voltage clamp. The currents have been compensated for membrane capacitance and background current using the P/4 protocol with a  $V_{\text{shp}}$  of  $-150$  mV. External and guard solutions contained 100 mM Na-methanesulfonate and internal solution contained 100 K-methanesulfonate. Data was digitized at  $5 \mu\text{s}$  per sample.  $V_h$  was  $-80$  mV. The  $V_i$  values were  $+50$  and  $-150$  mV. (A) Presteady-state currents in 100 mM  $[\text{Na}^+]_o$ . Current trace at  $+50$  mV was averaged from 10 sweeps. The other records were single sweeps. (B) Presteady-state currents 0  $[\text{Na}^+]_o$ . The records were single sweeps. Current and time scales are the same for A and B. (C)  $\tau$ - $V$  relations for fast charge. Data is from the experiment of A and B ( $V_h = -80$  mV). The filled symbols are from the ON, and open symbols from the OFF response. The circles (●) are obtained from the decay of the presteady-state current with hyperpolarizing pulses in 100 mM  $[\text{Na}^+]_o$ . The triangles (▲) were from the rising phase of the presteady-state current with depolarizing pulses and were obtained using a two exponential fit with the constraint that the time constant of decay was the same as those obtained from the same oocyte with 100-ms pulses. The squares (■) are the time constants of current decay in the absence of  $\text{Na}^+$ .

## Part II. Fluorescence Changes

**Slow Fluorescence Changes.** The time course of rhodamine fluorescence for a 100-ms voltage pulse using the two-electrode voltage clamp is shown in Fig. 7 A for TMR6M-labeled Q457C in 100 mM  $[\text{Na}^+]_o$ . There was a change of fluorescence intensity ( $\Delta F$ , a decrease for depolarizing and an increase for hyperpolarizing voltages) that returned to the holding level at the end of the pulse. The larger the voltage step, the larger was the  $\Delta F$ , but the time constant  $\tau$  was  $\approx 10$  ms and independent of voltage (see Loo et al., 1998; Meinild et al., 2002). With longer (500 ms) pulses, we observed an additional component (Fig. 7 B). In Fig. 7 B, the 100-ms records (from Fig. 7 A) were split (at 100 ms) and overlaid on the 500-ms records to agree at the onset of the ON and OFF pulses. The dashed traces indicate the  $\Delta F$  at 100 ms, and a comparison with the fluorescence level at 500 ms shows that the amplitude of the slow component increased with the size of the test voltage step in both depolarizing and hyperpolarizing directions. The amplitude of the slow component during the OFF response increased with the duration of the ON pulse, indicating that the slow component developed sequentially after relaxation of the 10-ms component.

The total fluorescence change ( $\Delta F_{\text{total}}$ ) was resolved into two components, slow ( $\Delta F_{\text{slow}}$ ) and medium

( $\Delta F_{\text{med}}$ ). To obtain  $\Delta F_{\text{slow}}$  and  $\Delta F_{\text{med}}$ , the  $\Delta F_{\text{total}}$  for the 500-ms pulse was fitted by a sum of two exponential components, and representative traces for the ON pulse are shown in Fig. 7 C for  $V_i = +90$  and  $-190$  mV. Time constant of this slow fluorescence ( $\tau_{\text{slow}}$ ) was independent of  $V_i$ ;  $\tau_{\text{slow}}$  was  $92 \pm 11$  ms ( $n = 7$ ) for the ON, and  $138 \pm 16$  ms ( $n = 10$ ) for the OFF pulses. For medium fluorescence, the time constant ( $\tau_{\text{med}}$ ) was also independent of voltage; between  $+50$  and  $-150$  mV,  $\tau_{\text{med}}$  was  $8.5 \pm 0.3$  ms ( $n = 10$ ) for ON and  $7.9 \pm 0.3$  ms ( $n = 10$ ) for OFF.

Fig. 7 D shows a plot of the amplitudes of  $\Delta F_{\text{slow}}$  and  $\Delta F_{\text{med}}$  vs. voltage. The  $\Delta F_{\text{med}}$ - $V$  relation was sigmoidal with a  $z\delta$  of 0.4 and  $V_{0.5}$  of  $-61$  mV. The slow component increased with the size of the voltage jump, but we were unable to obtain a Boltzmann fit to the  $\Delta F_{\text{slow}}$ - $V$  relation because of the low amplitudes and scatter. Nevertheless, inspection of the OFF records (Fig. 7 B) suggests that  $V_{0.5}$  is similar for the slow and medium components, i.e., the symmetry between the OFF responses to depolarizing and hyperpolarizing test pulses is similar for the medium and slow component. The maximal observed fluorescence change, the difference between the  $\Delta F$ 's at the largest depolarizing and hyperpolarizing voltages ( $+90$  and  $-190$  mV), was much larger for  $\Delta F_{\text{med}}$  than  $\Delta F_{\text{slow}}$  (ratio was  $\approx 5$ ). The sum of the two components,  $\Delta F_{\text{total}}$ , gave a  $z\delta$  of 0.4 and  $V_{0.5}$  of  $-61$  mV (Fig. 7 D).

**Q457C**  
**100 mM Na**

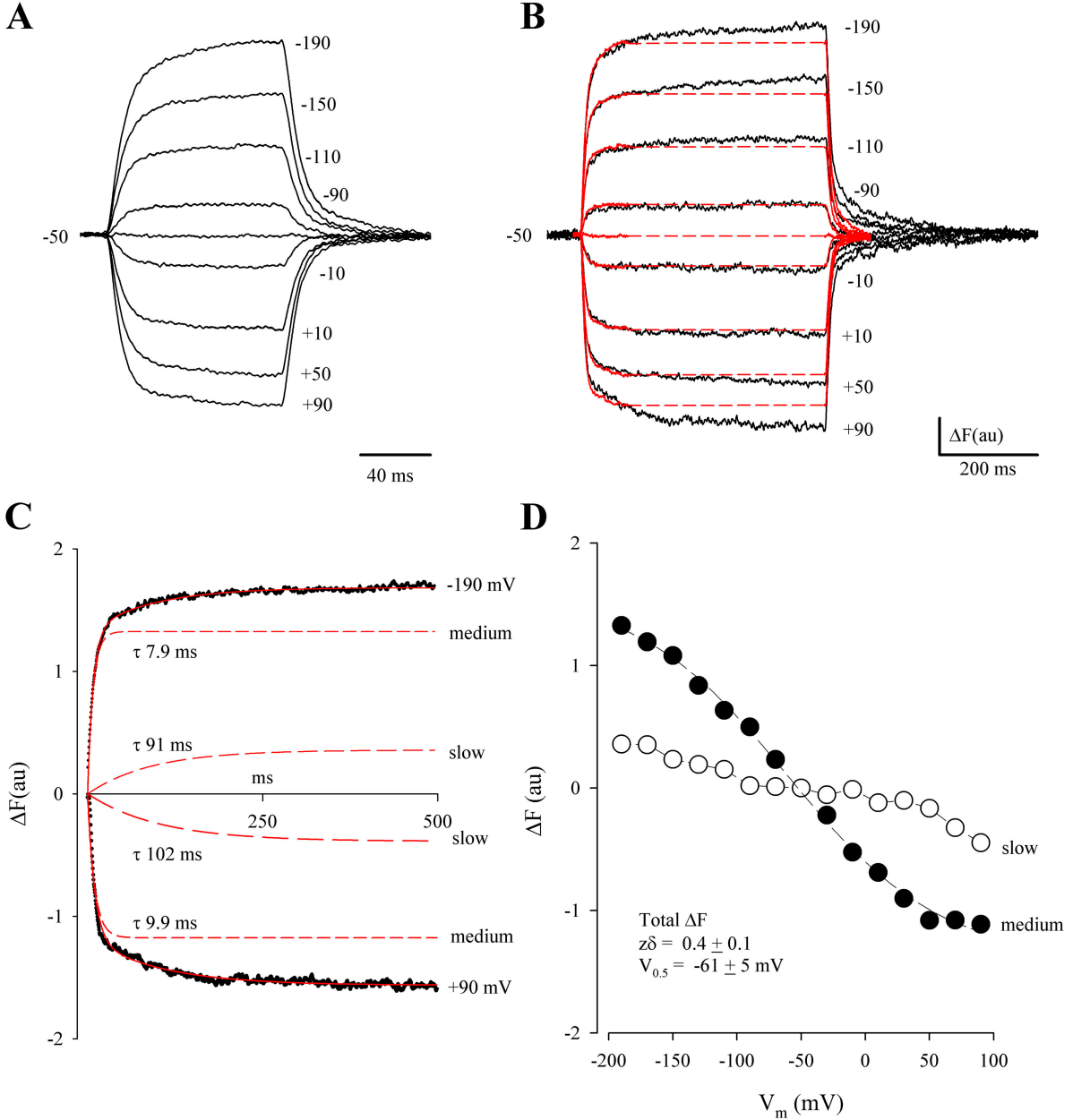


**FIGURE 7.** Slow ( $\Delta F_{\text{slow}}$ ) and medium ( $\Delta F_{\text{med}}$ ) components of  $\Delta F$ . The experiment was performed using a two-electrode voltage clamp on a TMR6M-labeled Q457C. Bath solution contained 100 mM  $\text{Na}^+$ . (A) Time course of  $\Delta F$  for a 100-ms pulse.  $V_h$  was  $-50$  mV and the  $V_t$  values are indicated next to the traces. (B) The corresponding  $\Delta F$  records for a 500-ms pulse, and superimposition of the short and long (100- and 500-ms) pulses. The traces from the 100-ms pulses (from A) have been split to overlap with the 500-ms pulses at the onset of the ON and OFF. The dotted lines indicate the  $\Delta F$  at 100 ms. (C)  $\Delta F_{\text{med}}$  and  $\Delta F_{\text{slow}}$ . The time course of total  $\Delta F$  (shown for  $V_t$  of  $+90$  and  $-190$  mV) was fitted (smooth curves) to two exponential components:  $\Delta F = \Delta F_{\text{med}} (1 - \exp(-t/\tau_{\text{med}})) + \Delta F_{\text{slow}} (1 - \exp(-t/\tau_{\text{slow}}))$ , where  $\Delta F_{\text{med}}$ ,  $\Delta F_{\text{slow}}$ ,  $\tau_{\text{med}}$ , and  $\tau_{\text{slow}}$  are the amplitudes and time constants of the medium and slow components. Parameters obtained from the fit were as follows: at  $+90$  mV,  $\Delta F_{\text{med}} = -1.17$  au,  $\tau_{\text{med}} = 9.9$  ms,  $\Delta F_{\text{slow}} = -0.38$  au,  $\tau_{\text{slow}} = 102$  ms; at  $-190$  mV,  $\Delta F_{\text{med}} = -1.33$  au,  $\tau_{\text{med}} = 7.9$  ms,  $\Delta F_{\text{slow}} = -0.36$  au,  $\tau_{\text{slow}} = 91$  ms. Dashed curves represent the  $\Delta F_{\text{med}}$  and  $\Delta F_{\text{slow}}$  components (from the fit) with the time constants next to the traces. The  $\tau$ 's were independent of  $V_t$  (between  $+50$  and  $-150$  mV).  $\tau_{\text{med}}$  was 7.9 ms and 8.5 ms ( $n = 10$ ) for the ON and OFF responses, respectively.  $\tau_{\text{slow}}$  ranged between 60 and 150 ms with a mean of 92 ms for the ON, and 138 ms for the OFF. (D)  $\Delta F_{\text{med}}-V$  (filled circles) and  $\Delta F_{\text{slow}}-V$  (open circles) relations.  $\Delta F$  (at each  $V_t$ ) was obtained from fitting the relaxation of  $\Delta F$  to two exponential components (as in C). The  $\Delta F_{\text{med}}-V$  and total  $\Delta F-V$  relations (sum of  $\Delta F_{\text{med}}$  and  $\Delta F_{\text{slow}}$ ) were fitted with the Boltzmann relation with  $\Delta F_{\text{max}} = 3.00 \pm 0.15$  au,  $z\delta = 0.4 \pm 0.1$ ,  $V_{0.5} = -61 \pm 4$  mV; and  $\Delta F_{\text{max}} = 3.86 \pm 0.24$  au,  $z\delta = 0.4 \pm 0.1$ ,  $V_{0.5} = -61 \pm 5$  mV.

The 100- and 500-ms fluorescence records at various  $[Na^+]_o$  are shown in Fig. 8 A. They are overlaid (as in Fig. 7 B). The slow component is evident at each  $Na^+$  concentration. The dependence of  $\Delta F_{med}$  on  $Na^+$  is shown in Fig. 8 B. The  $\Delta F_{med}$ -V relations obeyed the Boltzmann relation.  $z\delta$  was 0.4 and independent of  $[Na^+]_o$ . As  $[Na^+]_o$  was reduced, there was no apparent change in maximal fluorescence ( $\Delta F_{med}^{max}$ ), but there was a shift of  $V_{0.5}$  to more negative values: from  $-30$  mV at 100 mM  $Na^+$  to  $-99$  mV at 25 mM  $Na^+$ . In  $Na^+$ -free solutions, the  $\Delta F_{med}$ -V curve did not saturate even at the most negative voltage applied ( $-150$  mV). When  $V_{0.5}$  was plotted against  $[Na^+]_o$ , the slope yielded a 100-mV shift in  $V_{0.5}$  per 10-fold decrease in  $Na^+$  concentration (unpublished data), indicating that in  $Na^+$ -free solutions, the  $V_{0.5}$  is more negative than  $-200$  mV. The dashed line represents the Boltzmann relation in the absence of  $Na^+$ , with  $V_{0.5}$  of  $-200$  mV,  $\Delta F_{max}$  of 1, and  $z\delta$  of 0.4. The close agreement with the  $Na^+$ -free data indicates that in  $Na^+$ , the medium fluorescence can be largely attributed to the empty transporter.

The ratio of the slow and medium components,  $\Delta F_{slow}^{max}/\Delta F_{med}^{max}$  (taken between  $+50$  and  $-150$  mV), was independent of  $[Na^+]_o$  (at 100, 50, 25, and 0 mM):  $0.20 \pm 0.03$  ( $n = 4$ ) for the ON, and  $0.18 \pm 0.03$  ( $n = 4$ ) for the OFF pulses. The time constants for  $\Delta F_{med}$  and  $\Delta F_{slow}$  were independent of voltage and  $[Na^+]_o$ .  $\tau_{med}$  was  $\approx 10$  ms, and  $\tau_{slow}$  was  $\approx 150$  ms (see legend of Fig. 8 B).

**Fast Fluorescence Changes.** A fast component of fluorescence was observed using the cut-open oocyte voltage clamp. This is illustrated in Fig. 9 A, which shows the time course of  $\Delta F$  in 100 mM  $[Na^+]_o$ . The experiment was performed on the same oocyte as Fig. 6 with membrane potential held at  $-80$  mV. With onset of the voltage pulse, there was a fast initial change of fluorescence. The kinetics became faster when  $Na^+$  was removed from the external solution (Fig. 9 C). In both  $Na^+$  and  $Na^+$ -free solutions, increasing the pulse duration to 40 ms revealed an additional component with a time constant  $\tau \approx 10$  ms (Fig. 9, B and D). The amplitude of  $\Delta F$  was dependent on  $[Na^+]_o$ ; maximal change of fluorescence (between  $+50$  and  $-150$  mV) decreased 64% (from 6.3 to 4.0 arbitrary units) when  $Na^+$  was removed (Fig. 9 D).

The time course of  $\Delta F$  could be fitted by two exponentials, and representative records (at  $V_t = +50$  and  $-150$  mV) are shown in Fig. 10 (A and B) (for the ON and OFF pulses). The numbers next to the traces are the time constants ( $\tau_{fast}$ ) of the fast component. In the absence of  $Na^+$ ,  $\tau_{fast}$  was  $\approx 0.4$  ms and increased to  $\approx 2.0$  ms in 100 mM  $Na^+$  (Fig. 10 A). For the OFF response,  $\tau_{fast}$  was also  $\approx 0.4$  ms in 0 mM  $Na^+$  (Fig. 10 B). In the presence of  $Na^+$ , the recovery from  $+50$  mV was considerably faster ( $\tau_{fast} \approx 0.4$  ms; Fig. 10 B) than the recov-

ery from  $-150$  mV (1.9 ms). Fig. 10 (C and D) shows the  $\tau_{fast}$ -V relations. In the absence of  $Na^+$ ,  $\tau_{fast}$  was voltage independent, and was  $0.35 \pm 0.04$  ms ( $n = 9$ ) for ON, and  $0.34 \pm 0.03$  ms ( $n = 9$ ) for OFF. In  $Na^+$ ,  $\tau_{fast}$  was  $1.7 \pm 0.8$  ms ( $n = 9$ ) and independent of voltage. For the OFF response,  $\tau_{fast}$  depended on  $V_t$ ; when  $V_t$  was more negative than  $V_{h1}$ ,  $\tau_{fast}$  was  $\approx 2$  ms ( $2.0 \pm 0.1$  ms,  $n = 5$ ), and when more positive,  $\tau_{fast}$  was smaller (e.g., 0.41 ms at  $+50$  mV).

The time constants of the medium component ( $\tau_{med} \approx 11$  ms) was independent of voltage and  $[Na^+]_o$  (for both ON and OFF pulses). The  $\Delta F$ -V relation for the fast component in the presence of  $Na^+$  (100 mM) was sigmoidal, and could be fitted by the Boltzmann relation with a  $z\delta$  of  $0.6 \pm 0.1$  and a  $V_{0.5}$  of  $-48 \pm 7$  mV (Fig. 11 A). The medium  $\Delta F$ -V curve in  $Na^+$  was also sigmoidal, but because of the small amplitude, there was a large uncertainty in the maximal fluorescence, steepness factor, and midpoint voltage ( $\Delta F_{max} = 3.8 \pm 1.9$  au;  $z\delta = 0.5 \pm 0.3$ ;  $V_{0.5} = -100 \pm 47$  mV). We were unable to fit the medium  $\Delta F$ -V relation in the absence of  $Na^+$ . Compared with the fast, the medium component was relatively insensitive to  $Na^+$  (Fig. 11 B). In the absence of  $Na^+$ , the fast and medium components were similar ( $\Delta F_{fast}^{max}/\Delta F_{med}^{max} \approx 1$ ), and the major role of  $Na^+$  was to increase the amplitude of the fast component ( $\Delta F_{fast}^{max}/\Delta F_{med}^{max} \approx 3.3$ ).

The total  $\Delta F$ -V relation, measured using 100-ms pulses with the cut-open oocyte voltage clamp, was described by the Boltzmann relation; in four experiments performed in 100 mM  $[Na^+]_o$ ,  $z\delta$  was  $0.4 \pm 0.1$  ( $n = 4$ ) and  $V_{0.5}$  was  $-51 \pm 17$  mV ( $n = 4$ ). This is consistent with the results on the medium fluorescence ( $\Delta F_{med}$ ) obtained using the two-electrode voltage clamp (Figs. 7 and 8).

### Part III. Correlation between Charge Movement and Fluorescence Changes

**Medium and Slow Charge and Fluorescence Changes.** The time course of slow charge and fluorescence in the presence of  $Na^+$  (100 mM) are compared in the experiment of Fig. 12 A. Shown are the records in response to 750-ms hyperpolarizing voltage pulses from  $-50$  mV ( $V_{h1}$ ) to  $-110$ ,  $-130$ , and  $-150$  mV. For  $\Delta F$ , the time constants (of the ON response) were 9 and 169 ms. For comparison of the slow components, the concurrent charge and fluorescence records were normalized to 75 and 750 ms. Within this interval, there was a close agreement between the two time courses. We were unable to compare slow charge and fluorescence at large depolarizing voltages (more positive than  $+10$  mV) because of the high endogenous chloride currents of the oocytes. In the absence of  $Na^+$ , there was also a fair agreement between slow charge and slow fluorescence (Fig. 12 B).

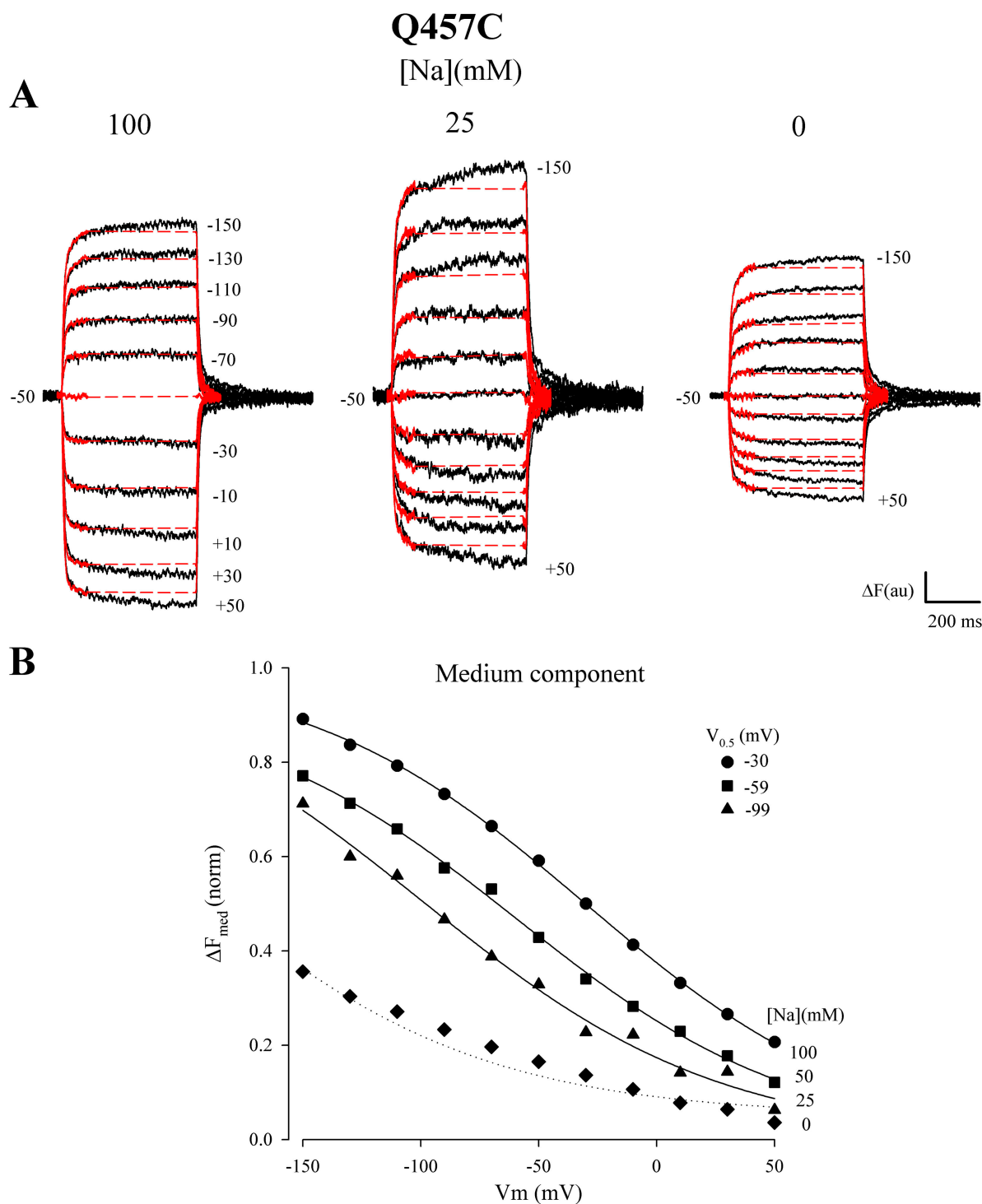
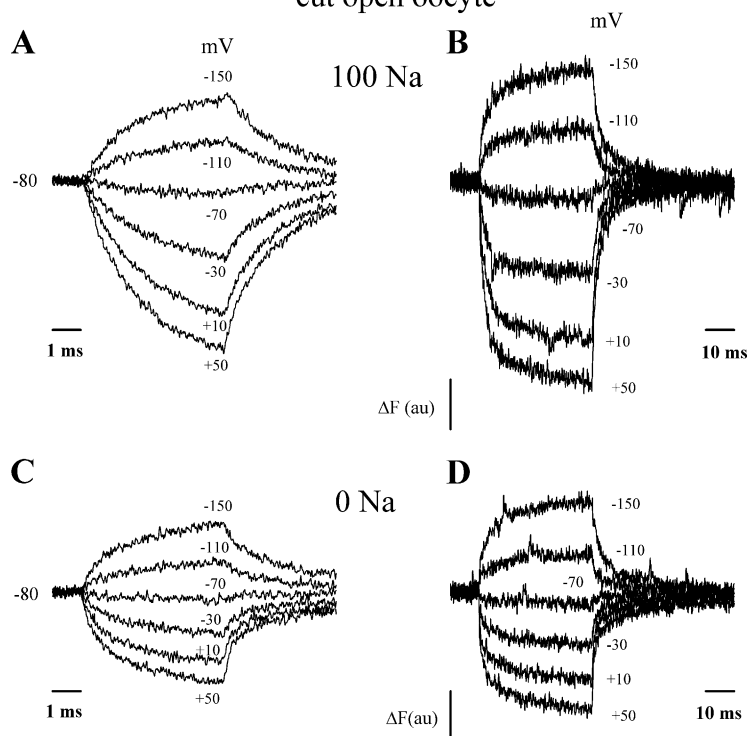


FIGURE 8. Dependence of the slow and medium components of  $\Delta F$  on  $[\text{Na}^+]_o$ . (A) Time course of  $\Delta F$  when  $[\text{Na}^+]_o$  was 100, 25, and 0 mM.  $[\text{Na}^+]_o$  was varied by choline replacement. The records from 100- and 500-ms pulses are overlaid, with the 100-ms records split (at 100 ms) to align with the 500-ms records at the onset of the ON and OFF pulses (see Fig. 7 B). Data were collected from a single oocyte, and all three panels share the abscissa and ordinate scales. The 500-ms records were fitted to  $\Delta F = \Delta F_{\text{med}}(1 - \exp(-t/\tau_{\text{med}})) + \Delta F_{\text{slow}}(1 - \exp(-t/\tau_{\text{slow}}))$ . The  $\tau$ 's obtained are independent of  $V_t$ . For ON, respectively at 100, 50, 25, and 0 mM  $[\text{Na}^+]_o$ ,  $\tau_{\text{med}}$  was  $11.6 \pm 0.2$  ms ( $n = 9$ ),  $11.4 \pm 0.3$  ms ( $n = 10$ ),  $11.3 \pm 0.4$  ms ( $n = 9$ ), and  $10.9 \pm 0.3$  ms ( $n = 10$ ); and  $\tau_{\text{slow}}$  was  $149 \pm 21$  ms ( $n = 7$ ),  $167 \pm 28$  ms ( $n = 6$ ),  $159 \pm 44$  ms ( $n = 6$ ), and  $146 \pm 22$  ms ( $n = 8$ ). For OFF,  $\tau_{\text{med}}$  was  $8.0 \pm 0.2$  ms ( $n = 10$ ),  $9.6 \pm 0.4$  ms ( $n = 10$ ),  $10.0 \pm 0.4$  ms ( $n = 9$ ), and  $10.2 \pm 0.4$  ms ( $n = 10$ ); and  $\tau_{\text{slow}}$  was  $154 \pm 41$  ms ( $n = 7$ ),  $184 \pm 38$  ms ( $n = 8$ ),  $119 \pm 45$  ms ( $n = 7$ ), and  $146 \pm 48$  ms ( $n = 7$ ). (B)  $\Delta F$ - $V$  relations for the medium component ( $\Delta F_{\text{med}}$ ).  $\Delta F_{\text{med}}$  and  $\Delta F_{\text{slow}}$  were obtained by curve fitting (described in A). At each  $[\text{Na}^+]_o$ , the  $\Delta F_{\text{med}}$ - $V$  curves were fitted (smooth curves) to the Boltzmann relation. At 100 mM  $[\text{Na}^+]_o$ ,  $z\delta = 0.4 \pm 0.03$ , and  $V_{0.5} = -30 \pm 3$  mV. At 50 mM  $[\text{Na}^+]_o$ ,  $z\delta = 0.4 \pm 0.07$ , and  $V_{0.5} = -59 \pm 6$  mV. At 25 mM  $[\text{Na}^+]_o$ ,  $z\delta = 0.4 \pm 0.15$ , and  $V_{0.5} = -99 \pm 31$  mV.

**Q457C**  
cut open oocyte



**FIGURE 9.** Fast fluorescence changes. Data was obtained using the cut-open oocyte on a TMR6M-labeled Q457C. External and guard solutions contained 100 mM Na-methanesulfonate and internal solution contained 100 mM K-methanesulfonate. Subtracting holding potential ( $V_{\text{shp}}$ ) was  $-150$  mV. The records were the averages of 20 sweeps. Data was digitized at  $5 \mu\text{s}$  per sample (A) and  $50 \mu\text{s}$  per sample (B). C and D show the time course of  $\Delta F$  in  $\text{Na}^+$ -free solution (choline replacement). Digitizing rate was  $5 \mu\text{s}$  per sample (C) and  $50 \mu\text{s}$  per sample (D).

Fig. 13 shows a comparison of medium components of charge and fluorescence (in a 75-ms pulse) in the presence of  $\text{Na}^+$  (100 mM). Since the time constant for charge was voltage dependent, while that for  $\Delta F$  was voltage independent (Fig. 4 A and Fig. 7C), one would anticipate a difference in time course between the two signals, and this is observed. In the depolarizing direction, charge ( $\tau \approx 4$  ms) led fluorescence ( $\tau \approx 8$  ms), and in the hyperpolarizing direction, fluorescence ( $\tau \approx 9$  ms) led charge ( $\tau \approx 21$  ms). This difference between charge and fluorescence in the medium component was also observed under  $\text{Na}^+$ -free conditions.

*Rising Phase of Charge Movement and Fluorescence.* The concurrent presteady-state current (I) and fluorescence records ( $\Delta F$ ) during the first 5 ms of a pulse from  $-80$  mV to  $+50$  mV are shown in Fig. 14 (from Figs. 6 and 9). In the presence of  $\text{Na}^+$ , with depolarizing pulses,  $\tau$  of the rising phase of charge movement was 0.17 ms while  $\tau$  of the fast fluorescence was 1.7 ms, indicating that “fast” charge (rising phase) led fast fluorescence. For hyperpolarizing pulses, charge also led fluorescence ( $\tau = 1.0$  ms for Q and 1.8 ms for  $\Delta F$ ; Table I). The presteady-state current was integrated to obtain the charge transferred. The charge transferred by the rising phase

(at 0.8 ms) was 21% of total charge transferred at the end of voltage pulse (at 5 ms) while the ratio of  $\Delta F$  at peak current (0.8 ms) to total  $\Delta F$  (at 5 ms) was 37%. This suggests that the fast component is responsible for the major change in the fluorescence signal, while the contribution of the rising phase to total charge was smaller. In the absence of  $\text{Na}^+$ , where  $\tau$  for fluorescence decreased to 0.4 ms, we were unable to detect a corresponding fast charge (Fig. 14 B), largely due to the low expression of the Q457C mutant in this oocyte.

#### DISCUSSION

Ion-driven cotransporters couple the transmembrane electrochemical potential gradient for ions ( $\text{Na}^+$  or  $\text{H}^+$ ) to the uphill transport of substrates. In recent years, evidence has been accumulating to indicate that all of these proteins share an alternating access mechanism; the initial step in energy transduction is the reorientation of the ligand-free binding sites from the internal to external membrane surface, and external cation binding. A common observation is the charge movements associated with these activation steps (for reviews see Forster et al., 2002; Loo et al., 2002).

For comparison, the curves have been normalized to the maximal extrapolated (slow-compensated) fluorescence change ( $\Delta F_{\text{max}}$ ) observed in 100 mM  $[\text{Na}^+]_o$ , and have also been shifted to align at the extrapolated depolarizing limit (see Loo et al., 1993; Meinild et al., 2001). The dotted line at 0  $\text{Na}^+$  was the Boltzmann relation with the same  $\Delta F_{\text{max}}$  and  $z\delta$  (0.4) as 100 mM  $[\text{Na}^+]_o$ , and  $V_{0.5}$  of  $-200$  mV.

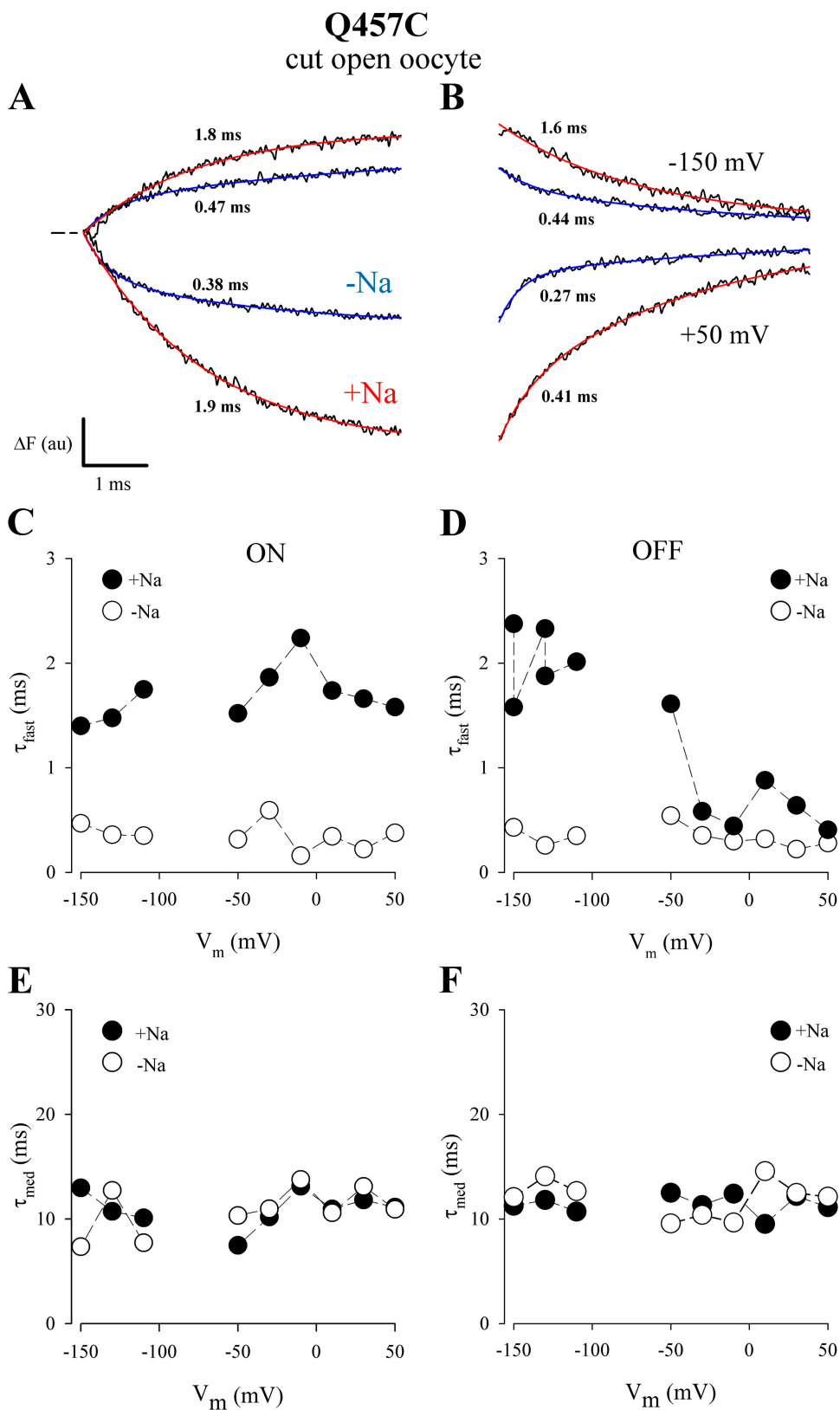


**FIGURE 10.** Voltage dependence of the fast and medium components of  $\Delta F$ . Time course of  $\Delta F$  (for a 5-ms pulse) at  $V_i$  of +50 and -150 mV ( $V_h = -80$  mV) in 100 mM  $[\text{Na}^+]_o$  (+Na) or 0  $\text{Na}^+$  (-Na). Data is from the experiment of Fig. 9. The fluorescence records were fitted to two exponential components (denoted by fast and medium). The number next to each trace is the time constant of the fast component ( $\tau_{\text{fast}}$ ). (C)  $\tau$ - $V$  relations for  $\tau_{\text{fast}}$  (ON). Open symbols (0  $\text{Na}^+$ ) were obtained from 5-ms pulses, and filled symbols (+Na) were from 40-ms pulses. (D)  $\tau$ - $V$  relations for  $\tau_{\text{fast}}$  (OFF). Data were from 5-ms pulses. (E and F)  $\tau$ - $V$  relations for  $\tau_{\text{med}}$  (for ON [E] and for OFF [F]). Data were from 40-ms pulses.

In the case of SGLT1, our previous studies have established that the distribution of the human isoform (hSGLT1) between two stable conformations,  $\text{Na}^+$ -

bound outward facing ( $C_2$ ) and the  $\text{Na}^+$ -free inward facing ( $C_6$ , Fig. 15 A), is voltage dependent. hSGLT1 charge movement as a function of membrane voltage is

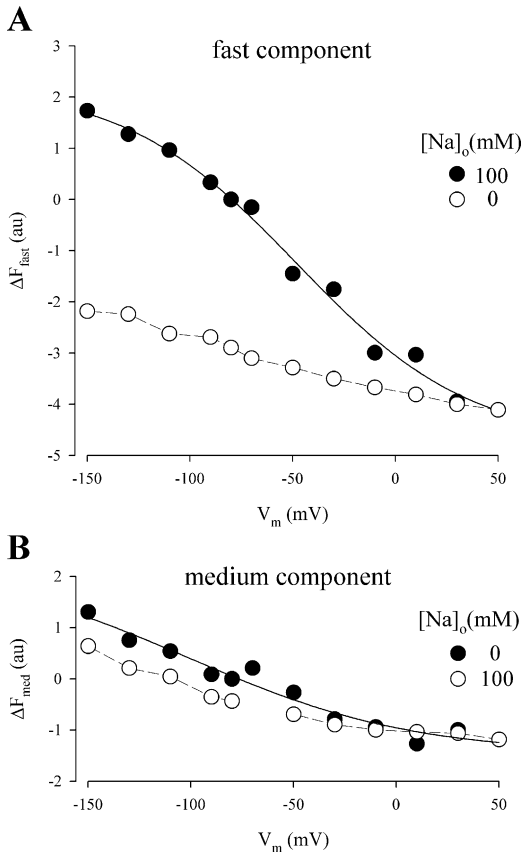


FIGURE 11.  $\text{Na}^+$  dependence of the fast and medium components of  $\Delta F$ . The fast and medium fluorescence amplitudes were obtained by fitting the time course of  $\Delta F$  to two exponential components (compare, Fig. 7). (A)  $\Delta F$ - $V$  relation for the fast component. The curve is the fit of the data in 100 mM  $\text{Na}^+$  to the Boltzmann relation with  $\Delta F_{\text{max}} = 7.0$  au,  $z = 0.6$ , and  $V_{0.5} = -48$  mV. The  $\Delta F$ - $V$  curve in 0  $\text{Na}^+$  has been shifted to align with that of 100 mM  $\text{Na}^+$  at +50 mV. (B)  $\Delta F$ - $V$  relation for the medium component. The curve is the fit of the data in 100 mM  $\text{Na}^+$  with  $\Delta F_{\text{max}} = 3.8 \pm 1.9$  au,  $z = 0.5 \pm 0.3$ , and  $V_{0.5} = -100 \pm 47$  mV. The  $\Delta F$ - $V$  curve in 0  $\text{Na}^+$  has been shifted to align with that of the 100 mM  $\text{Na}^+$  at +50 mV.

described by a Boltzmann relation with a  $V_{0.5}$  of  $\approx -50$  mV (Loo et al., 1993; Quick et al., 2001). The voltage dependence of the  $C_2$ - $C_6$  distribution was independently confirmed with optical studies of hSGLT1 (Loo et al., 1998; Meinild et al., 2002). Here we have expanded the study of the transitions between  $C_2$  and  $C_6$  using a voltage perturbation protocol where we monitored SGLT1 charge and fluorescence from microseconds to seconds. The resolution of our previous voltage clamp experiments on SGLT1 expressed in oocytes has been limited due to the speed of the clamp ( $\approx 1$  ms) and the limited duration of the voltage pulse (typically 100 ms). We now have recorded transients that have revealed hitherto unexpected features of the transitions between  $C_2$  and  $C_6$ , and these provide new insights into the partial reactions of the transporter. Confidence in

the new charge recordings is enhanced by the concurrent optical recordings since fluorescence measurements are subject to different constraints than charge measurements; charge is extracted from SGLT1 capacitive currents within a background of plasma membrane capacitive currents, SGLT1 ionic currents (uniporter currents), and membrane leakage currents (Parent et al., 1992; Loo et al., 1999), whereas SGLT1 optical records are measured against a constant background fluorescence (Loo et al., 1998; Meinild et al., 2002).

#### Multiple Components of Charge Movement and Fluorescence

A summary of the fast, medium and slow components of charge and fluorescence with time scales ranging from 0.2 to 200 ms is presented in Table I.

#### Charge Movement

*Slow Charge.* Whereas previous studies (Loo et al., 1993; Hazama et al., 1997; Quick et al., 2001) have documented SGLT1 charge movement between  $C_2$  and  $C_6$  with time constants in the range 2–20 ms (medium component), we now have clearly demonstrated an additional slow component with time constants in the range of 100 ms (Fig. 4 A; Table I). The slow charge movements were found in the presence and absence of  $\text{Na}^+$  (Fig. 12, A and B), indicating that they are associated with the unloaded carrier. A major consequence of this new slow component is that we have previously overestimated the turnover rate of SGLT1. The turnover rate is estimated from the ratio ( $I_{\text{max}}/Q_{\text{max}}$ ) of the maximal rate of sugar transport ( $I_{\text{max}}$ ) and maximal charge ( $Q_{\text{max}}$ ). Previous estimates for human SGLT1,  $57 \text{ s}^{-1}$ , were based on the medium component (Loo et al., 1993). Since the total charge ( $Q_{\text{max}}$ ) is doubled with inclusion of the slow component, the turnover rate of human SGLT1 is reduced by 50%, to  $28 \text{ s}^{-1}$ .

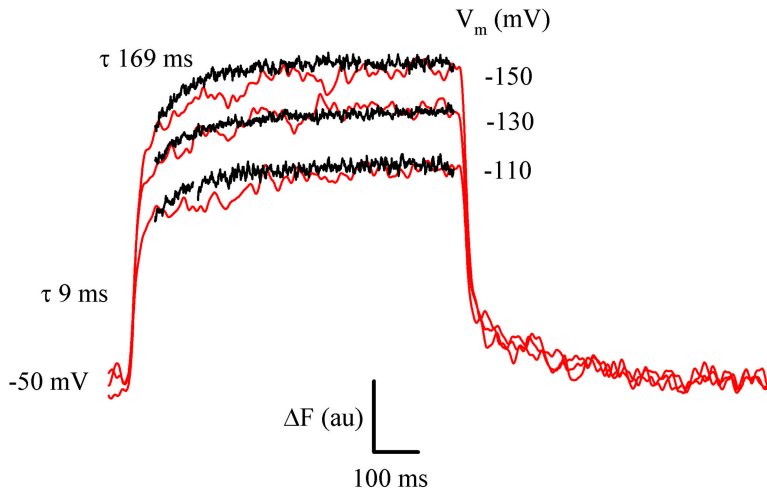
Our finding of a slow charge (in the presence and absence of  $\text{Na}^+$ ) in human SGLT1 is consistent with reports of time constants up to 50 ms in rabbit SGLT1 (Krofchick and Silverman, 2003). Since the rabbit currents were obtained from 100-ms pulses, they are undoubtedly underestimated (Krofchick and Silverman, 2003). In long pulse protocols on rabbit SGLT1, we have found that the slow component required  $\approx 80$  ms at +20 mV and  $\approx 500$  ms at -100 mV to reach steady state (unpublished data).

The time constants of the slow component (Table I) has important operational consequences for the protocol used in charge movement studies; i.e., the test voltage pulses need to be separated by interpulse intervals greater than five times the slowest time constant (or  $\approx 500$  ms). This may, in part, explain the variations in the kinetics of charge movement observed using different protocols (present study; Chen et al., 1996; Krofchick and Silverman, 2003).

# Q457C

100 mM Na

**A**



**B**

0 Na

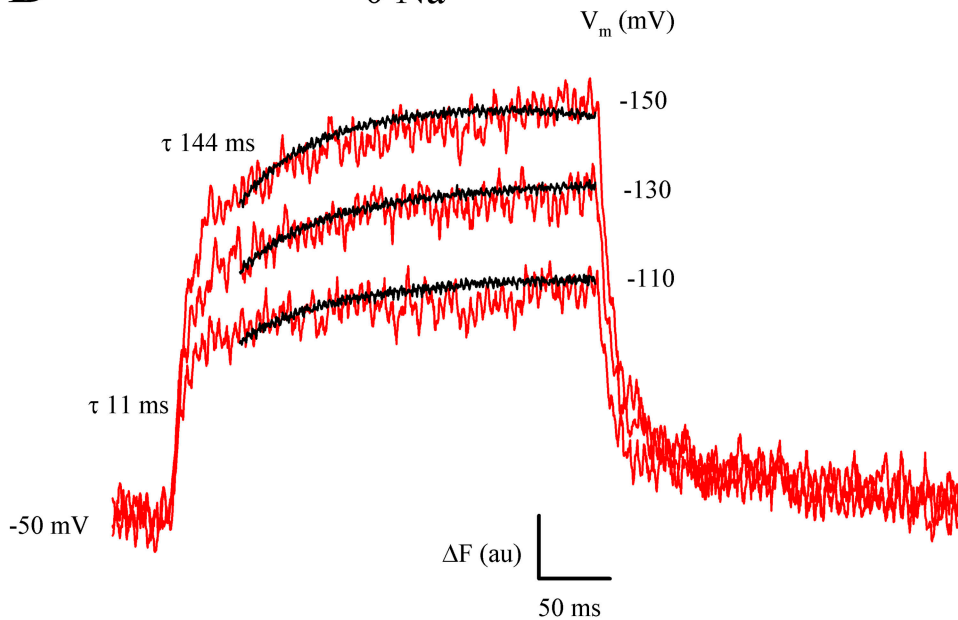


FIGURE 12. Correlation between slow charge and fluorescence. Experiment was performed using a two-electrode voltage clamp on TMR6M Q457C. (A) Correlation between slow charge and fluorescence (red traces) in 100 mM  $[Na^+]_o$ . The charge record has been normalized to agree with  $\Delta F$  at 40 and 750 ms. Shown are records at hyperpolarizing voltages of  $-110$ ,  $-130$ , and  $-150$  mV from  $V_h = -50$  mV.  $\Delta F$  contained two voltage-independent time constants of  $9 \pm 1$  ms ( $n = 10$ ) and  $169 \pm 19$  ms ( $n = 7$ ) for the ON, and  $9 \pm 1$  ms ( $n = 10$ ) and  $154 \pm 9$  ms ( $n = 9$ ) for the OFF response.  $\tau_{slow}$  for charge (ON) was  $104 \pm 10$  ms ( $n = 3$ ). (B) Correlation between slow charge and slow fluorescence in  $Na^+$ -free solution. Pulse duration was 300 ms, and  $V_h$  was  $-50$  mV. The current records have been normalized to agree with the fluorescence at 50 and 300 ms (as in A).  $\Delta F$  (for the ON pulse) contained two voltage-independent time constants of  $11 \pm 1$  ms ( $n = 8$ ) and  $144 \pm 15$  ms ( $n = 8$ ).  $\tau_{slow}$  for charge (ON) was  $63 \pm 8$  ms ( $n = 3$ ).

*Medium Charge.* The medium charge, with  $\tau$  between 3 and 35 ms (Table I), has been previously described for human, rabbit, and rat SGLT1 (Loo et al., 1993, 1998; Panayotova-Heiermann et al., 1995; Chen et al., 1996; Hazama et al., 1997; Quick et al., 2001; Meinild et al., 2002; Krofchick and Silverman 2003; Krofchick et al., 2004). In the present study, the current records for the medium component (for hSGLT1 and TMR6M-labeled hSGLT1 Q457C) were corrected for the slow component (Fig. 2, A and C), and the  $\tau$ - $V$  and  $Q$ - $V$  relations obtained are similar to those described previously on

hSGLT1 and the TMR6M-labeled hSGLT1 Q457C from uncorrected records (Loo et al., 1993; Chen et al., 1996; Hirayama et al., 2001; Quick et al., 2001; Meinild et al., 2002). In the case of the rabbit isoform, the time constant for medium charge can be simulated by the kinetic model for SGLT1 (Hazama et al., 1997).

The slow and medium charge movements were equal in magnitude (Fig. 4, B and C). Their time constants showed similar voltage dependences; they were voltage independent for hyperpolarizing voltages and decreased with depolarizing voltages (Fig. 4 A). For both



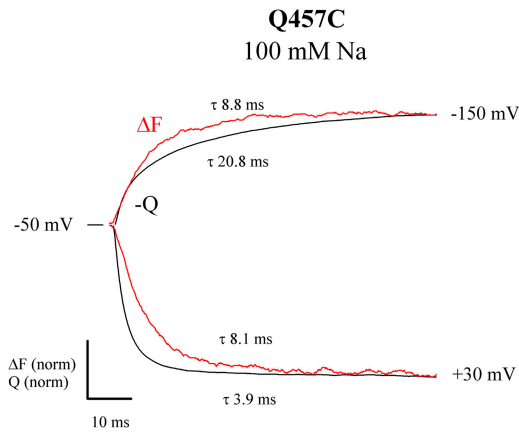


FIGURE 13. Correlation between medium charge and fluorescence. Experiment was performed using a two-electrode voltage clamp on a TMR6M-labeled Q457C in 100 mM NaCl buffer.  $V_h$  was  $-50$  mV. The time course of  $Q$  and  $\Delta F$  are compared at  $+30$  and  $-150$  mV.  $Q$  was obtained from the total current by subtraction of the steady-state current and the oocyte membrane capacitive transient. The traces have been normalized to agree at the end of the voltage pulse (75 ms). The numbers next to the traces are the time constants of  $Q$  and  $\Delta F$ .

ON and OFF,  $z\delta$  was identical between medium and slow charge, but  $V_{0.5}$  was  $-33$  mV for medium and  $-67$  mV for slow. The total charge vs. voltage ( $Q$ - $V$ ) relation was described by a Boltzmann function with two states and a single steepness factor ( $z\delta$ ) of 1.0. Since total charge consists of three components, the  $Q$ - $V$  relation could, in principle, be fitted by a Boltzmann function with four states. Chen et al. (1996) obtained a  $z\delta$  of 0.7–0.8 for human SGLT1 (in 90 mM  $[\text{Na}^+]_o$ ), and as slow charge was not reported, this represented the sum of the fast and medium components. Krofchick et al. (2004) modeled the  $Q$ - $V$  relation of rabbit SGLT1 (for total charge with fast, medium, and slow components) by a Boltzmann function with three states (and two steepness factors) and obtained  $z\delta$  values of 0.45 and 0.97 and  $V_{0.5}$  values of  $-7$  and  $-49$  mV. A proper analysis of Boltzmann distributions with multiple states requires experimental protocols that take into account the range of the time constants.

**Fast Charge.** Our previous consideration of fast hSGLT1 charge movements, i.e., components with time constants  $<2$  ms, have been fraught with uncertainty due to large membrane capacitive transients with a time constant of  $\approx 0.5$  ms. This has been clarified by use of the phlorizin subtraction protocol (Fig. 5, A and B) and the cut-open oocyte voltage clamp with a settling time of 80  $\mu\text{s}$  (Fig. 6). We observed two components of fast charge: (1) a fast decay for hyperpolarizing pulses in the presence of  $\text{Na}^+$ , and both hyperpolarizing and depolarizing voltage pulses in the absence of  $\text{Na}^+$ ; and (2) a rising phase with large depolarizing pulses in the presence of  $\text{Na}^+$ . As will be discussed (below), these fast

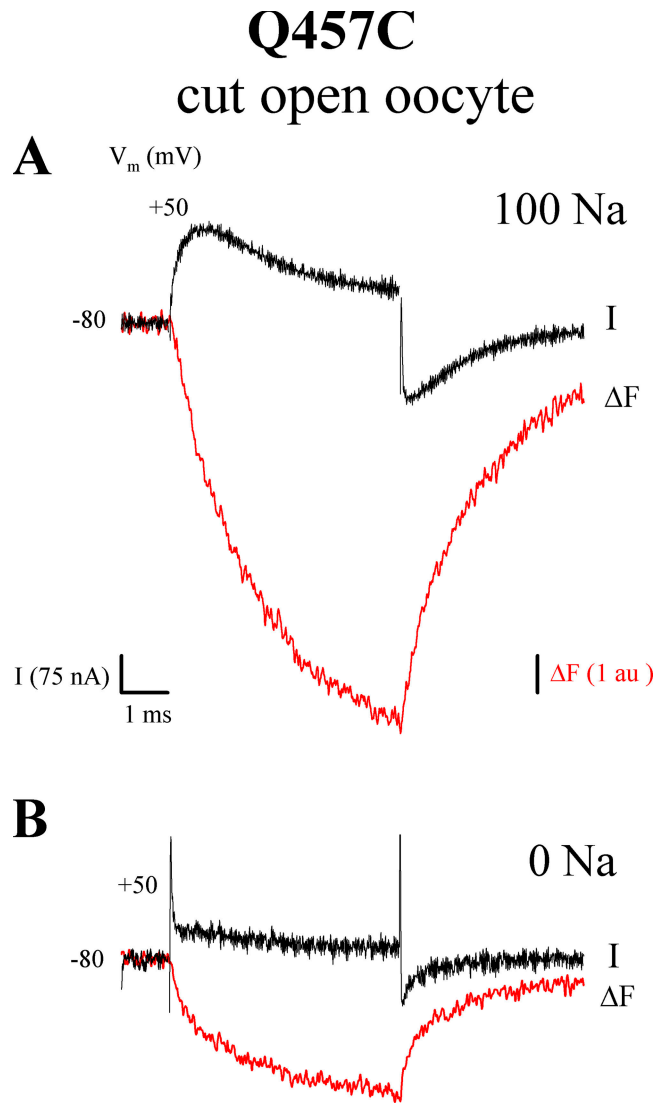


FIGURE 14. Correlation between fast charge and fluorescence. The experiment was performed using the cut-open oocyte on TMR6M-labeled Q457C (from the oocyte of Fig. 6). Membrane potential was held at  $-80$  mV and stepped to  $+50$  mV. (A) Comparison of the rising phase of the presteady-state current ( $I$ ) and fluorescence ( $\Delta F$ ) in 100 mM  $[\text{Na}^+]_o$ .  $I$  is from Fig. 6 A and  $\Delta F$  is from Fig. 9 A. (B) Comparison of charge and  $\Delta F$  in absence of  $\text{Na}^+$ .  $I$  is from Fig. 6 B and  $\Delta F$  is from Fig. 9 C.

components indicate that there are two fast conformational changes of hSGLT1 between  $C_2$  and  $C_6$  (Fig. 15), and the dominant component depends on the experimental condition. The time constant of the fast decay is 0.2–1.5 ms for ON, and 1.6 ms for OFF (Table I). A fast decay (with  $\tau \approx 0.4$ –0.8 ms in the presence and absence of  $\text{Na}^+$ ) has been reported by Chen et al. (1996) using the cut-open oocyte, and suggested by Krofchick and Silverman (2003;  $\tau \approx 0.5$ –1.0 ms) using phlorizin subtraction and two-electrode voltage clamp.

The fast rising phase is a novel finding of this study. The time constant was 200  $\mu\text{s}$ ,  $\text{Na}^+$  dependent and volt-

T A B L E I

Summary of the Time Constants for Charge Movement and Fluorescence for TMR6M-labeled hSGLT1 Q457C

|               | $\tau_{ON}$ (ms)   |                 |                    |                 | $\tau_{OFF}$ (ms) |                      |                 |                 |
|---------------|--------------------|-----------------|--------------------|-----------------|-------------------|----------------------|-----------------|-----------------|
|               | Depolarizing       |                 | Hyperpolarizing    |                 | Depolarizing      |                      | Hyperpolarizing |                 |
|               | Q                  | $\Delta F$      | Q                  | $\Delta F$      | Q                 | $\Delta F$           | Q               | $\Delta F$      |
| +Na           |                    |                 |                    |                 |                   |                      |                 |                 |
| $\tau_{slow}$ | $30 \pm 1^{a\#}$   | $149 \pm 21$    | $104 \pm 10$       | $149 \pm 21$    | $99 \pm 4$        | $54 \pm 41$          | $99 \pm 4$      | $49 \pm 21$     |
| $\tau_{med}$  | $4 \pm 1^{\#}$     | $12 \pm 1$      | $19 \pm 1$         | $12 \pm 1$      | $15 \pm 1$        | $8 \pm 1$            | $15 \pm 1$      | $12 \pm 1$      |
| $\tau_{fast}$ | $0.17 \pm 0.01^b$  | $1.7 \pm 0.8$   | $1.3 \pm 0.1$      | $1.7 \pm 0.1$   | $1.7 \pm 0.1$     | $0.41 \pm 0.02^{\#}$ | $1.7 \pm 0.1$   | $2.0 \pm 0.1$   |
| -Na           |                    |                 |                    |                 |                   |                      |                 |                 |
| $\tau_{slow}$ | ND                 | $146 \pm 22$    | $63 \pm 8$         | $146 \pm 22$    | ND                | $46 \pm 48$          | $63 \pm 8$      | $146 \pm 48$    |
| $\tau_{med}$  | $1.9 \pm 0.1^{\#}$ | $11 \pm 1$      | $3.5 \pm 0.1^{\#}$ | $11 \pm 1$      | $2.4 \pm 0.1$     | $10 \pm 1$           | $2.4 \pm 0.1$   | $10 \pm 1$      |
| $\tau_{fast}$ | $0.24 \pm 0.01$    | $0.35 \pm 0.04$ | $0.24 \pm 0.01$    | $0.35 \pm 0.04$ | $0.17 \pm 0.01$   | $0.34 \pm 0.03$      | $0.17 \pm 0.01$ | $0.34 \pm 0.03$ |

$\tau_{ON}$  for depolarizing and hyperpolarizing potentials were determined in the presence 100 mM  $Na^+$  or absence of  $Na^+$  at  $V_i$  of +50 mV, and -150 mV.  $\tau_{OFF}$  was determined when  $V_i$  was returned to  $V_h$  (-50 or -80 mV) from +50 (depolarizing) and -150 mV (hyperpolarizing). These are the means and standard errors of three to nine estimates, except those indicated by #, which are the errors of the fit for individual experiments, but these were repeated on at least three oocytes. ND, not determined.

<sup>a</sup>For hSGLT1 (not determined for TMR6M-labeled Q457C).

<sup>b</sup>For the rising phase of charge movement in TMR6M-labeled Q457C.

age independent (Fig. 5 B; Fig. 6 B). Hints of a rising phase have been observed experimentally in human SGLT1 using the two-electrode voltage clamp (Loo et al., 1993) and in model simulations for rabbit SGLT1 (Hazama et al., 1997). The rising phase has not been reported by other investigators, largely because kinetics were studied using conditioning prepulses of only 40 ms (Chen et al., 1996) and with hyperpolarizing pulses and/or with OFF responses (Chen et al., 1996; Krofchick and Silverman, 2003). The rising phase has confounded our attempts to estimate the contribution of fast charge to total charge. A lesson gained from the present study is that given the wide range of time scales, for kinetic studies, voltage pulses of different durations need to be applied and extra caution taken to ensure that steady-state conditions are reached for accurate estimation of presteady-state kinetics.

*Dependence of Charge on  $Na^+$ .* The kinetics of charge movement was dependent on external  $Na^+$ . With decreasing  $[Na^+]$ , there was a shift of Q-V curve. For example, for the medium component,  $V_{0.5}$  shifted negative ( $\approx 100$  mV/10-fold reduction in  $[Na^+]_o$ ) with no change in  $z\delta$  (Loo et al., 1993, Fig. 3; Hazama et al., 1997, Fig. 3; Quick et al., 2001, Fig. 3 B). There was little change in maximal charge ( $Q_{max}$ ) until  $[Na^+]$  was below 25 mM (Loo et al., 1993, Fig. 3; Hazama et al., 1997, Fig. 3; Quick et al., 2001, Fig. 3 B). In the absence of  $Na^+$ , there was an apparent loss of charge (Fig. 5, A, B, and D) due to the shift of the Q-V curve out of working range (between -150 and +50 mV). The medium charge observed was 50% of that observed in 100 mM  $Na^+$  (Fig. 5 D).

The time constants for all three components of charge decreased with  $[Na^+]$  (Table I). For example, as  $[Na^+]$  is reduced from 100 to 0 mM, for fast decay,  $\tau$  de-

creased from 1.6 to 0.2 ms (Fig. 6 C); for medium charge,  $\tau$  decreased from 14 to 3 ms (Fig. 5 C); and for slow charge,  $\tau$  decreased from 104 to 63 ms. For the rising phase with depolarizing pulses, the time to peak decreased with reducing  $[Na^+]$ , in part due to a decrease in the time constant of the medium component (Fig. 5 B).

#### Q457C-TMR6M Fluorescence

Similar to charge, there were three components of fluorescence (Table I): slow ( $\tau$  100 ms), medium (10 ms), and fast (1 ms). The maximal fluorescence ( $\Delta F_{max}$ ) of the slow component was 20% of the medium. The fast fluorescence was extracted from the medium using the cut-open oocyte preparation (Fig. 10), and the dependence of medium fluorescence on  $[Na^+]$  observed in two-electrode voltage experiments (Fig. 8 B) was actually due to the  $Na^+$  sensitivity of the fast component (Fig. 11 A). Since  $\Delta F_{max}$  for fast fluorescence increased threefold between 0 and 100 mM  $Na^+$  (Fig. 11 A), we estimate that in 100 mM  $Na^+$ , 60% of the total  $\Delta F$  was fast, 20% medium, and 20% slow. In contrast,  $\approx 50\%$  of the total charge was medium and  $\approx 50\%$  slow (fast charge was small). Thus there is a small charge associated with a large change in fast fluorescence.

In  $Na^+$ ,  $V_{0.5}$  was -48 mV for the fast (Fig. 11 A), and  $-100 \pm 50$  mV (Fig. 7 B and Fig. 11 B) for the medium and slow components of fluorescence. For medium and fast fluorescence,  $z\delta$  was  $\approx 0.4$  (see Fig. 4, Meinild et al., 2002; Fig. 7 D; Fig. 11), and the time constants for all three components of fluorescence were voltage independent, with  $\tau_{ON}$  and  $\tau_{OFF}$  generally equal (Fig. 10; Table I). We were unable to precisely determine the Boltzmann parameters for the slow component, largely due to the low expression of this mutant.

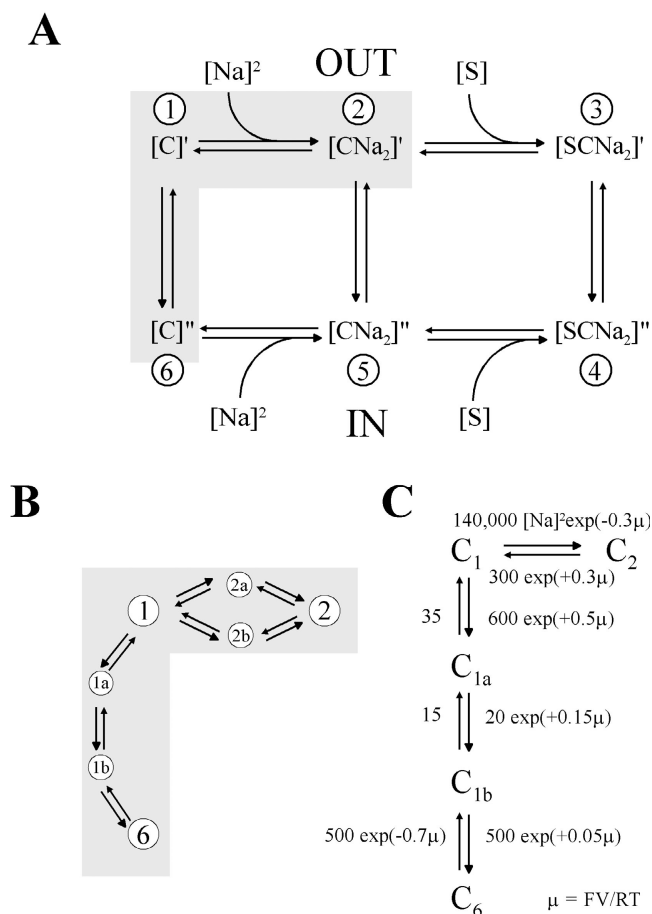


FIGURE 15. Kinetic model for  $\text{Na}^+$ /glucose cotransport (modified from Parent et al., 1992). (A) The transporter has six kinetic states consisting of the empty transporter C (states  $C_1$  and  $C_6$ ), the  $\text{Na}^+$ -bound  $\text{CNa}_2$  (states  $C_2$  and  $C_5$ ) and the  $\text{Na}^+$ - and sugar-bound  $\text{SCNa}_2$  (states  $C_3$  and  $C_4$ ) in the external and internal membrane surfaces. Two  $\text{Na}^+$  ions bind to the transporter before the sugar molecule. The shaded region represents the voltage-dependent steps: conformational change of the empty transporter between the external and internal membrane surfaces ( $C_1 \leftrightarrow C_6$ ); and  $\text{Na}^+$  binding/dissociation ( $C_1 \leftrightarrow C_2$ ). The simplifying assumption (for high external  $[\text{Na}^+]$ ) is that the two  $\text{Na}^+$  binding steps are lumped into one. The distribution of the conformations depends on membrane voltage. The transporter is in  $C_2$  at large hyperpolarizing voltages, and  $C_6$  at large depolarizing voltages. In the TMR6M-labeled Q457C, sugar transport is abolished, and since  $\text{Na}^+$  binding/dissociation at the cytoplasmic surface may be neglected because internal  $[\text{Na}^+]$  is low and internal  $\text{Na}^+$  binding constant is high (see MATERIALS AND METHODS), only the partial reactions in the shaded area are studied. (B) Seven-state model for presteady-state current.  $C_{1a}$  and  $C_{1b}$  represent intermediate states between  $C_1$  and  $C_6$ , and  $C_{2a}$  and  $C_{2b}$  are the states with one  $\text{Na}^+$  bound. The rate constants ( $k_{ij}$ ) for transition between two states ( $C_i \rightarrow C_j$ ) are defined by  $k_{ij} = k_{ij}^0 \exp(-\varepsilon_{ij}FV/RT)$ , where  $k_{ij}^0$  is a voltage-independent rate,  $\varepsilon_{ij}$  is the voltage dependency, and F, R, and T have their usual physicochemical meanings. (C) A simplified five-state kinetic model for charge movement and the assumptions on the rate constants that were used for the simulation described in Fig. 16.

$\Delta F$  as a Function of  $\text{Na}^+$ . The time constants for fluorescence showed some dependence on  $\text{Na}^+$ . For the slow component,  $\tau$  was 169 ms vs. 144 ms in  $\text{Na}^+$  free (Table I). For medium component,  $\tau$  was 19 ms in presence and absence of  $\text{Na}^+$ . For the fast component,  $\tau$  was 1.5 ms vs. 0.2 ms in  $\text{Na}^+$  free. Charge and fluorescence changes as a function of  $\text{Na}^+$  suggest that most if not all charge and fluorescence changes are due to conformational changes of the unloaded carrier, i.e.,  $C_1$ - $C_6$  transitions. A more thorough investigation of the fast transients was made possible by the fluorescence experiments. In the absence of  $\text{Na}^+$ , there was a fast component of the fluorescence,  $\tau \approx 300$ - $500 \mu\text{s}$ , that is independent of voltage (Fig. 10 C), but the ON response is slowed by the presence of external  $\text{Na}^+$  to 2 ms (Fig. 10 C). This observation is consistent with the  $\text{Na}^+$  dependence of the rising phase of charge movement (Fig. 6 C). A fast component of the fluorescence change,  $\tau \approx 400 \mu\text{s}$  is nevertheless observed for the OFF response in  $\text{Na}^+$ , but only for the depolarizing voltage pulses (Fig. 10 D).

#### Charge vs. Fluorescence Measurements

Charge and fluorescence measurements provide complementary views of the global/local conformational changes. The following observations indicate that to each charge state, there is a corresponding fluorescence state, and a closely associated conformational change to each component of charge movement: (a) the  $V_{0.5}$  for total charge ( $\approx -50$  mV) was similar to that for total fluorescence (present study; Meinild et al., 2002); (b) the shift of the  $V_{0.5}$  with varying  $[\text{Na}^+]$ ,  $-100$  mV/10-fold reduction in  $[\text{Na}^+]$ , was the same for charge as for fluorescence (present study; Meinild et al., 2002); (c) the time constants of each component of charge movement were in the same range as those for fluorescence; and (d) the time constants of fast charge and fluorescence showed a decrease with reducing  $[\text{Na}^+]$ .

The major difference between charge and fluorescence measurements was their dependence on voltage. (a) For the voltage dependence of the Boltzmann relation,  $z\delta$  was 0.4 for fluorescence vs. 1.0 for charge. (b) We have found that  $z\delta$ , which provides a measure of the voltage dependence of the global protein conformations, was the same ( $\approx 1$ ) for SGLT1 mutants (unpublished data). On the other hand,  $z\delta$  for fluorescence, which depended on the local environment of the fluorophore, depended on the location of TMR6M; e.g.,  $z\delta$  for medium fluorescence of TMR6M-labeled D454C was 0.6 (Díez-Sampedro et al., 2004). (c) The time constants for charge were voltage dependent (for medium and slow components), while those for fluorescence were voltage independent. We do not yet understand the mechanism whereby the time con-

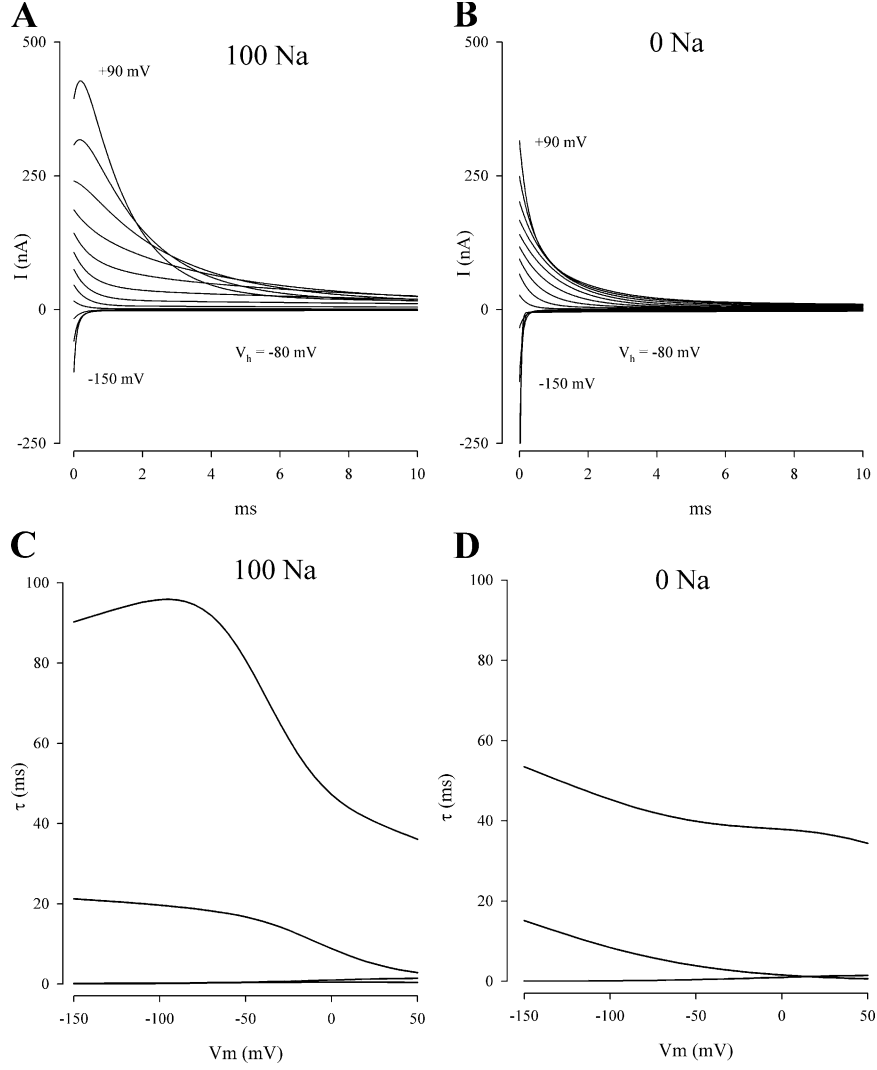


FIGURE 16. A model simulation for the presteady-state currents (A and B) and  $\tau$ - $V$  relations (C and D) in 100 and 0 mM external  $[\text{Na}^+]$ . Simulations were performed on the kinetic scheme:  $C_2 \leftrightarrow C_1 \leftrightarrow C_{1a} \leftrightarrow C_{1b} \leftrightarrow C_6$  using the assumptions and rate constants summarized in Fig. 15 C. The simulation was performed with the membrane potential held at  $-80$  mV at  $20^\circ\text{C}$ , and the voltage pulses (between  $+90$  and  $-150$  mV in 20 decrements) were applied for 10 to 500 ms. The differential equation relating the time evolution of states was solved numerically at each test voltage using Berkeley Madonna. The equation is

$$\frac{d}{dt} \begin{bmatrix} C_2 \\ C_1 \\ C_{1a} \\ C_{1b} \\ C_6 \end{bmatrix} = - \begin{bmatrix} -k_{21} & k_{12} & 0 & 0 & 0 \\ k_{21} & -(k_{12} + k_{11a}) & k_{1a1} & 0 & 0 \\ 0 & k_{11a} & -(k_{1a1b} + k_{1a1}) & k_{1b1a} & 0 \\ 0 & 0 & k_{1a1b} & -(k_{1b1a} + k_{1b6}) & k_{61b} \\ 0 & 0 & 0 & k_{1b6} & -k_{61b} \end{bmatrix} \begin{bmatrix} C_2 \\ C_1 \\ C_{1a} \\ C_{1b} \\ C_6 \end{bmatrix}.$$

The sum of the occupancy probabilities in all the states is 1 ( $C_1 + C_2 + C_{1a} + C_{1b} + C_6 = 1$ ). For simulation, the total number of transporters in the oocyte plasma membrane was  $5 \times 10^9$  transporters (Zampighi et al., 1995). There are four components of charge movement ( $C_2 \leftrightarrow C_1$ ,  $C_1 \leftrightarrow C_{1a}$ ,  $C_{1a} \leftrightarrow C_{1b}$ , and  $C_{1b} \leftrightarrow C_6$ ), and associated with each transition ( $C_i \leftrightarrow C_j$ ) the charge ( $I_{ij}$ ) was calculated by  $I_{ij} = e(\epsilon_{ij} + \epsilon_{ji})(k_{ij}C_i - k_{ji}C_j)$ , where  $e$  is the elementary charge,  $\epsilon_{ij}$  is the voltage dependence, and  $k_{ij}$  is the rate constants for transition from  $C_i$  to  $C_j$  (see also Krofchick and Silverman, 2003). The eigenvalues (which are reciprocals of the time constants) of the matrix were obtained using MATLAB 6.0 (The MathWorks Inc.).

stants of the fluorescence changes were independent of voltage but the steady-state  $\Delta F$ - $V$  relations were voltage dependent.

While there was good agreement between the time course of charge and fluorescence for the fast and slow components (in the hyperpolarizing direction), there

was a difference in the medium component (Fig. 13); in the hyperpolarizing direction, fluorescence led charge movement, indicating that the change in local environment of the fluorophore at residue 457 preceded the conformational changes that generate the charge movement. The situation is reversed in the depolarizing direction with charge movement leading fluorescence. These differences between charge and fluorescence depended on the location of the fluorophore on the protein. Preliminary experiments on mutant protein hSGLT1 I443C (labeled with TMR6M) indicated a close agreement between charge and fluorescence for depolarizing and hyperpolarizing pulses (unpublished data). Further studies on the relation between charge movement and fluorescence at different locations in the protein may enable us to obtain a spatial and temporal map of the conformational changes of the cotransporter.

Concurrent charge and fluorescence experiments have been performed on the glucose (Loo et al., 1998; Meinild et al., 2002),  $\gamma$ -aminobutyric acid (GAT1; Li et al., 2000), serotonin (SERT; Li and Lester, 2002), and glutamate transporters (EAAT3; Larsson et al., 2004), and the general agreement between charge and fluorescence and their dependence on substrates confirmed, in real time, that conformational changes are involved in transporter function. These studies have also revealed differences between charge and fluorescence, e.g., there were fluorescence changes in GAT1 (Li et al., 2000), SERT (Li and Lester, 2002), and EAAT3 (Larsson et al., 2004) without a corresponding charge movement. In SGLT1, the changes in the local environment at residue 457C (as monitored by fluorescence) closely mirrored the global conformational changes of the protein.

The slow time constant for SGLT1 is in the range for the  $\text{Na}^+/\text{Cl}^-/\text{GABA}$  family, such as GAT1 (Mager et al., 1993, 1996; Loo et al., 2000; Whitlow et al., 2003). The turnover rate is comparable to the turnover rate for SGLT1, indicating that reorientation of the empty transporter is the rate-limiting step for both families of cotransporters.

#### *Kinetic Model for $\text{Na}^+/\text{Glucose}$ Cotransport*

In the absence of external glucose and low internal  $[\text{Na}^+]_i$ , the six-state model for  $\text{Na}^+/\text{sugar}$  cotransport is reduced to the three-state model for charge movement, and the three-state model accounted qualitatively for the medium  $Q-V$  (Boltzmann) and  $\tau-V$  relations, and the shift of these relations with reducing  $[\text{Na}^+]_o$  (Fig. 5, C and D; Loo et al., 1993; Hazama et al., 1997). The model also predicted a rising phase of charge movement with depolarization at high  $[\text{Na}^+]_o$  (Hazama et al., 1997). A rising phase is developed when the charge transfer associated with the empty carrier ( $C_1 \leftrightarrow C_6$ ) is

faster and greater than the charge associated with  $\text{Na}^+$  binding/dissociation ( $C_2 \leftrightarrow C_1$ ).  $\text{Na}^+$  binding/dissociation is apparently the slower step because of the fast "back" reaction of  $\text{Na}^+$  binding ( $C_2 \leftarrow C_1$ ). In absence of  $\text{Na}^+$ , the "back" reaction is absent, and the rising phase is not observed. This also explains the decrease of the time to peak of the medium component as external  $[\text{Na}^+]_o$  is reduced (Fig. 5 B). The rising phase is not observed at hyperpolarizing voltages because the fastest charge is moved during the first step ( $C_6 \rightarrow C_1$ ).

A rising phase has been observed in the gating currents of Shaker  $\text{K}^+$  channels (Bezanilla et al., 1991; Stefani et al., 1994). Like the charge movement of SGLT1, the development depended on membrane voltage; the rising phase was not observed for small depolarizations ( $\approx 20$  mV) from the holding potential ( $-80$  mV), but became pronounced with large depolarization voltages more positive than  $+50$  mV (Fig. 1 of Bezanilla et al., 1991). The development of the rising phase (of charge movement) in SGLT1 and (gating current) in Shaker  $\text{K}^+$  channels is due to the increase in the rate of charge transfer with positive membrane voltages and the majority of the charge being carried by the later step (Bezanilla et al., 1991; Parent et al., 1992; Loo et al., 1993; Stefani et al., 1994; Hazama et al., 1997).

A simplifying assumption of the three-state model (for  $C_2-C_6$  transitions) involves the  $\text{Na}^+$  binding step; the two  $\text{Na}^+$  binding reactions ( $C_1 + \text{Na}^+ \leftrightarrow C_1\text{Na}$ ;  $C_1\text{Na} + \text{Na}^+ \leftrightarrow C_2$ ) are lumped into one,  $C_1 + 2\text{Na}^+ \leftrightarrow C_2$  (Hazama et al., 1997; Parent et al., 1992; Loo et al., 1993). This one-step approximation at high  $[\text{Na}^+]_o$  is supported by the observation of high cooperativity between the two  $\text{Na}^+$  binding sites (Parent et al., 1992; Falk et al., 1998; Mackenzie et al., 1998; Meinild et al., 2002). However, the simplified model runs into difficulties when external  $[\text{Na}^+]_o$  is lowered. The model predicted a smaller shift of the  $V_{0.5}$  with reducing  $[\text{Na}^+]_o$  than experimentally observed (Hazama et al., 1997). In computer modeling, Falk et al. (1998) found that replacement of the two  $\text{Na}^+$  binding steps by a single step results in a  $\text{Na}^+$ -dependent pseudo rate constant from  $C_1$  to  $C_6$ , and this leads to incorrect predictions as external  $[\text{Na}^+]_o$  is reduced. Thus for low  $\text{Na}^+$  concentrations, the two  $\text{Na}^+$  binding steps need to be included.

In view of the additional fast and slow components of charge observed in the absence of  $\text{Na}^+$  (for a total of three time constants), the single step transition between  $C_1$  and  $C_6$  needs to be extended. Two additional intermediate states (in addition to end states  $C_1$  and  $C_6$ ) are required for the empty transporter:  $C_1 \leftrightarrow C_{1a} \leftrightarrow C_{1b} \leftrightarrow C_6$ . Together with the binding of two  $\text{Na}^+$  ions to  $C_1$  to form  $C_2$  a total of at least seven states are required to describe the presteady-state kinetics of SGLT1 (Fig. 15 B). Thus, in saturating  $[\text{Na}^+]_o$  at hyperpolarizing voltages (eg.,  $-150$  mV) where there is

a high occupancy in  $C_2$ , when membrane voltage is stepped to large positive values, the protein goes through more than three intermediate states before reaching  $C_6$  ( $C_{2a}$ ,  $C_{2b}$ ,  $C_1$ ,  $C_{1a}$ ,  $C_{1b}$ ). The estimation of 16 rate constants (each with unknown voltage dependences [ $z\delta$ 's]) for a total of 32 parameters) of a seven-state kinetic scheme is a formidable task.

Our computer simulations suggest that with the current knowledge no one set of kinetic parameters can account for the charge movement between  $C_2$  and  $C_6$ . In order to illustrate the simulations we present one example in Fig. 15 C. Here we make the assumptions that (a) the two sodium ions bind to the transporter in one step; (b) the rates of the conformational changes are fast ( $C_2 \leftrightarrow C_1$ ), medium ( $C_1 \leftrightarrow C_{1a}$ ), slow ( $C_{1a} \leftrightarrow C_{1b}$ ) and fast ( $C_{1b} \leftrightarrow C_6$ ); (c) all the transitions from  $C_2$  to  $C_6$  are voltage dependent; and (d) for transitions from  $C_6$  to  $C_2$ , only the first ( $C_6 \rightarrow C_{1b}$ ) and last ( $C_1 \rightarrow C_2$ ) steps are voltage dependent. Fig. 16 A shows the predicted charge movements in 100 mM  $\text{Na}^+$  for 10-ms voltage pulses ranging from  $-80$  ( $V_h$ ) to  $+90$  and  $-150$  mV, and Fig. 16 C shows the time constants as a function of the test potential. Four components of charge are predicted: two fast and difficult to discriminate between, and medium and slow components with voltage dependencies similar to those observed experimentally (compare Fig. 4 A). The fast components (0.2–2 ms) are relatively insensitive to voltage. The medium component has time constants decreasing from 25 to 3 ms from  $-150$  to  $+50$  mV. The slow component has time constants ranging from 90 to 25 ms from  $-150$  to  $+50$  mV. A rising phase is also predicted for depolarizing voltage steps with a peak current at 0.5 ms. In the absence of  $\text{Na}^+$ , the rising phase is not present. Only three components of charge are predicted, and there is a decrease in the time constants for the medium and slow components (Fig. 16, C and D). It can also be deduced from Fig. 16 (A and B) that on removing  $\text{Na}^+$ , the  $V_{0.5}$  for charge movement does not shift to the measured value ( $-200$  mV). The failure of the model to predict the change in  $V_{0.5}$ , similar to the failure of the three-state model (Hazama et al., 1997), is likely due to our assumption that the binding of two  $\text{Na}^+$  ions can be represented as a single rate constant (see also Falk et al., 1998).

This simulation does produce transient currents that are quite similar to those observed in Fig. 4 A, Fig. 5 (A and C), and Fig. 6 C. However, a clear discrepancy is noted between the simulation and the experimental results concerning the onset of the rising phase and the shape of the peak. Experimentally, the rising current originates from zero and the peak is broad (Fig. 6 A), whereas in the simulation, the current does not originate from zero and the peak is sharp (Fig. 16 A). The probable origin of this discrepancy is the assumption

about the binding of the two  $\text{Na}^+$  ions in one step, and this is becoming a focus of future research.

Our assumptions about the relative rates of the conformational transitions of the empty carrier (from  $C_1 \rightarrow C_{1a} \rightarrow C_{1b} \rightarrow C_6$ ) are an extension of our original two-state model (Hazama et al., 1997) and the three-state models proposed by Chen et al. (1996) and Krofchick and Silverman (2003) to account for the fast and medium charge movements. Both of the latter groups postulated an intermediate state  $C_{1a}$  between  $C_1$  and  $C_6$  to account for the fast charge in the absence of  $\text{Na}^+$ , and a medium transition between  $C_1$  and  $C_{1a}$ . Our results require an additional intermediate  $C_{1b}$  and a slow transition between  $C_{1a}$  and  $C_{1b}$ .

The simulation in Fig. 16 also makes the following predictions. (a) The observed asymmetry of voltage dependence of the forward and backward reactions of the transitions between  $C_1$  and  $C_6$ . The medium and slow conformational changes are voltage dependent in the depolarizing direction ( $C_1 \rightarrow C_{1a} \rightarrow C_{1b}$ ) but voltage independent in the hyperpolarizing direction ( $C_1 \leftarrow C_{1b} \leftarrow C_{1a}$ ). This is consistent with our assumption that for transitions from  $C_1$  to  $C_6$ , the major voltage-dependent step (major charge movement) is  $C_1 \rightarrow C_{1a}$ , and for transitions from  $C_6$  to  $C_1$ , the major voltage-dependent step is  $C_6 \rightarrow C_{1b}$ .

(b) In the presence of  $\text{Na}^+$ , the system behaves energetically as though it has two equilibrium states,  $C_2$  and  $C_6$ . This suggests that  $C_1$ ,  $C_{1a}$ , and  $C_{1b}$  are unstable intermediates or states with extremely low occupancy. The instability of  $C_1$  is also supported by our previous findings that in the absence of  $\text{Na}^+$ , the estimated  $V_{0.5}$  values for the medium  $Q$ - $V$  and  $\Delta F$ - $V$  relations are  $\approx -200$  mV (Meinild et al., 2002). Stabilization of the unloaded carrier in the outward-facing conformation by the activating cation ( $\text{Na}^+$  or  $\text{H}^+$ ) appears to be a common mechanism for ion-coupled transporters, e.g., the  $\text{Na}^+/\text{Cl}^-/\gamma$ -aminobutyric acid (GAT1; Hilgemann and Lu, 1999),  $\text{H}^+$ /dipeptide (PEPT1; Mackenzie et al., 1996), glutamate (EAAT; Wadiche et al., 1995),  $\text{Na}^+/\text{P}_i$  cotransporter (NaP<sub>i</sub>; Forster et al., 2002), and  $\text{H}^+$ /lactose transporters (Abramson et al., 2003).

(c) The rising phase of charge movement is due to the transition  $C_2 \rightarrow C_1 \rightarrow C_{1a}$ . The implication is that the charge associated with the  $C_1$  to  $C_{1a}$  transition is greater than that with the dissociation of  $\text{Na}^+$ ,  $C_2 \rightarrow C_1$ . The observation of a rising phase (with large depolarizing steps) requires that the major charge be associated with the empty transporter.

(d) A charge associated with  $\text{Na}^+$  binding/dissociation. This is not observed experimentally, although it is indicated in the simulation (compare Fig. 15, A and C). This suggests that the predicted charge is either extremely fast, within 80  $\mu\text{s}$  (settling time of the cut-open oocyte voltage clamp), or that the amount of charge as-

sociated with this step is very small (beyond the resolution of the current measurements).

### Conclusions

Our application of perturbation methods to SGLT1 by recording charge and fluorescence signals upon step jumps in membrane voltage have permitted the study of partial reactions of the transport cycle. In the absence of sugar and  $\text{Na}^+$ , we have obtained evidence for four states ( $C_1$ ,  $C_{1a}$ ,  $C_{1b}$ , and  $C_6$ ). Transitions between  $C_1$  and  $C_6$  carried most of the charge, and are the major voltage-dependent steps in the overall  $\text{Na}^+$ /glucose cotransport cycle.  $C_1$ ,  $C_{1a}$  and  $C_{1b}$  are unstable conformations. Transitions between  $C_1$  and  $C_6$  contribute the most to charge and  $\Delta F$  measurements, i.e., the major voltage-dependent step in the overall transport cycle is the "return" of the unloaded carrier between the interior and exterior surfaces of the membrane. The kinetic states (obtained from charge movement studies) are also supported by the fluorescence measurements.

In general, TMR6M bound to Q457C exhibited fluorescence changes with a time course similar to charge movement. This suggests that global conformational changes monitored by charge movement are reflected by conformational changes at or near Q457C. However, there are subtle differences: the local conformations occurred BEFORE charged transitions from  $C_6$  to  $C_2$  and AFTER charged transitions from  $C_2$  to  $C_6$ . Finally, the combination of charge and fluorescence recordings at different locations in the protein may be used to construct a spatial map of the conformational changes of the transporter.

Major unresolved questions include the charge associated with  $\text{Na}^+$  association and dissociation with the transporter (very fast and/or very small), the order of the binding and dissociation of the two  $\text{Na}^+$  ions, and the nature of the cooperativity between the two  $\text{Na}^+$  binding sites. Resolving these issues has important implications for both the kinetics of SGLT1 charge movement and the kinetics of  $\text{Na}^+$ /glucose cotransport.

We thank E. Gallardo, D. Leung, M. Lai-Bing, A. Johnson, and K. Edwards for the preparation, injection, and care of oocytes, and Dr. Dan Sigg for valuable discussions on fast charge movements.

This research was supported by National Institutes of Health grant DK19567.

Olaf S. Andersen served as editor.

Submitted: 15 July 2004

Accepted: 2 November 2004

### REFERENCES

Abramson, J., I. Smirnova, V. Kasho, G. Verner, H.R. Kaback, and S. Iwata. 2003. Structure and mechanism of the lactose permease of *Escherichia coli*. *Science*. 301:610–615.

Bezanilla, F., and C.M. Armstrong. 1977. Inactivation of the sodium channel. I. Sodium current experiments. *J. Gen. Physiol.* 70:549–

566.

Bezanilla, F., and E. Stefani. 1998. Gating currents. *In Methods in Enzymology*. Vol. 293, Ion Channels, Part B. P.M. Conn, editor. Academic Press, New York. 331–352.

Bezanilla, F., E. Perozo, D.M. Papazian, and E. Stefani. 1991. Molecular basis of gating charge immobilization in *Shaker* potassium channels. *Science*. 254:679–683.

Cha, A., and F. Bezanilla. 1997. Characterizing voltage-dependent conformational changes in the *Shaker*  $\text{K}^+$  channel with fluorescence. *Neuron*. 19:1127–1140.

Cha, A., and F. Bezanilla. 1998. Structural implications of fluorescence quenching in the *Shaker*  $\text{K}^+$  channel. *J. Gen. Physiol.* 112: 391–408.

Chen, X.-Z., M.J. Coady, and J.-Y. Lapointe. 1996. Fast voltage clamp discloses a new component of presteady-state currents from the  $\text{Na}^+$ -glucose cotransporter. *Biophys. J.* 71:2544–2552.

Díez-Sampedro, A., D.D.F. Loo, E.M. Wright, and B.A. Hirayama. 2004. Coupled sodium-glucose cotransport by SGLT1 requires a negative charge at position 454. *Biochemistry*. 43:13175–13184.

Eskandari, S., D.D.F. Loo, and E.M. Wright. 1999. Functional asymmetry of the sodium/glucose cotransporter. *FASEB J.* A399 (Abstr).

Falk, S., A. Guay, C. Chenu, S.D. Patil, and A. Berteloot. 1998. Reduction of an eight-state mechanism of transport to a six-state model using a new computer program. *Biophys. J.* 74:816–830.

Forster, I.C., K. Kohler, J. Biber, and H. Murer. 2002. Forging the link between structure and function of electrogenic cotransporters: the renal type IIa  $\text{Na}^+$ / $\text{P}_i$  cotransporter as a case study. *Prog. Biophys. Mol. Biol.* 80:69–108.

Hazama, A., D.D.F. Loo, and E.M. Wright. 1997. Presteady-state currents of the  $\text{Na}^+$ /glucose cotransporter (SGLT1). *J. Membr. Biol.* 155:175–186.

Hilgemann, D.W., and C.-C. Lu. 1999. GAT1 ( $\text{GABA}:\text{Na}^+:\text{Cl}^-$ ) cotransport function: database reconstruction with an alternating access model. *J. Gen. Physiol.* 114:459–475.

Hirayama, B.A., A. Diez-Sampedro, and E.M. Wright. 2001. Common mechanisms of inhibition for the  $\text{Na}^+$ /glucose (hSGLT1) and  $\text{Na}^+/\text{Cl}^-/\text{GABA}$  (hGAT1) cotransporters. *Br. J. Pharmacol.* 134:484–495.

Krofchick, D., S.A. Huntley, and M. Silverman. 2004. Transition states of the high-affinity rabbit  $\text{Na}^+$ /glucose cotransporter SGLT1 as determined from measurement and analysis of voltage-dependent charge movements. *Am. J. Physiol. Cell Physiol.* 287: C46–C54.

Krofchick, D., and M. Silverman. 2003. Investigating the conformational states of the rabbit  $\text{Na}^+$ /glucose cotransporter. *Biophys. J.* 84:3690–3702.

Larsson, H.P., A.V. Tzingounis, H.P. Koch, and M.P. Kavanaugh. 2004. Fluorometric measurements of conformational changes in glutamate transporters. *Proc. Natl. Acad. Sci. USA*. 101:3951–3956.

Li, M., R.A. Farley, and H.A. Lester. 2000. An intermediate state of the  $\gamma$ -aminobutyric acid transporter GAT1 revealed by simultaneous voltage clamp and fluorescence. *J. Gen. Physiol.* 115:491–508.

Li, M., and H.A. Lester. 2002. Early fluorescence signals detect transitions at mammalian serotonin transporters. *Biophys. J.* 83:206–218.

Loo, D.D.F., S. Eskandari, K.J. Boorer, H.K. Sarkar, and E.M. Wright. 2000. Role of  $\text{Cl}^-$  in electrogenic  $\text{Na}^+$ -coupled cotransporters GAT1 and SGLT1. *J. Biol. Chem.* 275:37414–17422.

Loo, D.D.F., S. Eskandari, B.A. Hirayama, and E.M. Wright. 2002. A kinetic model for secondary active transport. *In IAMS Volumes in Mathematics and its Applications*. Volume 129. A. Weinstein and H. Layton, editors. Springer Verlag, New York. 65–83.

Loo, D.D.F., A. Hazama, S. Supplisson, E. Turk, and E.M. Wright.

1993. Relaxation kinetics of the Na<sup>+</sup>/glucose cotransporter. *Proc. Natl. Acad. Sci. USA*. 90:5767–5771.
- Loo, D.D.F., B.A. Hirayama, E.M. Gallardo, J.T. Lam, E. Turk, and E.M. Wright. 1998. Conformational changes couple Na<sup>+</sup> and glucose transport. *Proc. Natl. Acad. Sci. USA*. 95:7789–7794.
- Loo, D.D.F., B.A. Hirayama, A.-K. Meinild, G. Chandy, T. Zeuthen, and E.M. Wright. 1999. Passive water and ion transport by cotransporters. *J. Physiol.* 518:195–202.
- Mackenzie, B., D.D.F. Loo, and E.M. Wright. 1998. Relationship between Na<sup>+</sup>/glucose cotransporter (SGLT1) currents and fluxes. *J. Membr. Biol.* 162:101–106.
- Mackenzie, B., D.D.F. Loo, Y. Fei, W.J. Liu, V. Ganapathy, F.H. Leibach, and E.M. Wright. 1996. Mechanisms of the human intestinal H<sup>+</sup>-coupled oligopeptide transporter hPEPT1. *J. Biol. Chem.* 271:5430–5437.
- Mager, S.J., N. Kleinberger-Dorn, G.I. Keshet, N. Davidson, B.I. Kanner, and H.A. Lester. 1996. Ion binding and permeation at the GABA transporter GAT1. *J. Neurosci.* 16:5405–5414.
- Mager, S., J. Naeve, M. Quick, C. Labarca, N. Davidson, and H.A. Lester. 1993. Steady-states, charge movements, and rates for a cloned GABA transporter expressed in *Xenopus* oocytes. *Neuron*. 10:177–188.
- Meinild, A.-K., B.A. Hirayama, E.M. Wright, and D.D.F. Loo. 2002. Fluorescence studies of ligand-induced conformational changes of the Na<sup>+</sup>/glucose cotransporter. *Biochemistry*. 41:1250–1258.
- Meinild, A.-K., D.D.F. Loo, B.A. Hirayama, E. Gallardo, and E.M. Wright. 2001. Evidence for the involvement of Ala 166 in coupling Na<sup>+</sup> to sugar transport through the human Na<sup>+</sup>/glucose cotransporter. *Biochemistry*. 40:11897–11904.
- Panayotova-Heiermann, M., D.D.F. Loo, and E.M. Wright. 1995. Kinetics of steady-state currents and charge movements associated with the rat Na<sup>+</sup>/glucose cotransporter. *J. Biol. Chem.* 270:27099–27105.
- Parent, L., S. Supplisson, D.D.F. Loo, and E.M. Wright. 1992. Electrogenic properties of the cloned Na<sup>+</sup>/glucose cotransporter: II. A transport model under nonrapid equilibrium conditions. *J. Membr. Biol.* 130:203.
- Quick, M., D.D.F. Loo, and E.M. Wright. 2001. Neutralization of a conserved amino acid residue in the human Na<sup>+</sup>/glucose transporter (hSGLT1) generates a glucose-gated H<sup>+</sup> channel. *J. Biol. Chem.* 276:1728–1734.
- Quick, M., J. Tomasevic, and E.M. Wright. 2003. Functional asymmetry of the human Na<sup>+</sup>/glucose transporter (hSGLT1) in bacterial membrane vesicles. *Biochemistry*. 42:9147–9152.
- Sauer, G.A., G. Nagel, H. Koepsell, E. Bamberg, and K. Hartung. 2000. Voltage and substrate dependence of the inverse transport mode of the rabbit Na<sup>+</sup>/glucose cotransporter (SGLT1). *FEBS Lett.* 469:98–100.
- Stefani, E., and F. Bezanilla. 1998. Cut-open oocyte voltage-clamp technique. In *Methods in Enzymology*. Vol. 298. Ion Channels, Part B. P.M. Conn, editor. Academic Press, New York. 300–318.
- Stefani, E., L. Toro, E. Perozo, and F. Bezanilla. 1994. Gating of *Shaker* K<sup>+</sup> channels: I. Ionic and gating currents. *Biophys. J.* 66:996–1010.
- Su, A., S. Mager, S.L. Mayo, and H.A. Lester. 1996. A multi-substrate single-file model for ion-coupled transporters. *Biophys. J.* 70:762–777.
- Tagliatalata, M., L. Toro, and E. Stefani. 1992. Novel voltage clamp to record small, fast currents from ion channels expressed in *Xenopus* oocytes. *Biophys. J.* 61:78–82.
- Umbach, J.A., M.J. Coady, and E.M. Wright. 1990. Intestinal Na<sup>+</sup>/glucose cotransporter expressed in *Xenopus* oocytes is electrogenic. *Biophys. J.* 57:1217–1224.
- Wadiche, J.I., J.L. Arriza, S. Amara, and M.P. Kavanaugh. 1995. Kinetics of a human glutamate transporter. *Neuron*. 14:1019–1027.
- Whitlow, R.D., A. Sacher, D.D.F. Loo, N. Nelson, and S. Eskandari. 2003. The anticonvulsant valproate increases the turnover rate of  $\gamma$ -aminobutyric acid transporters. *J. Biol. Chem.* 278:17716–17726.
- Zampighi, G.A., M. Kreman, K.J. Boorer, D.D.F. Loo, F. Bezanilla, G. Chandy, J.E. Hall, and E.M. Wright. 1995. A method for determining the unitary functional capacity of cloned channels and transporters expressed in *Xenopus laevis* oocytes. *J. Membr. Biol.* 148:65–78.